J. Fluid Mech. (1967), *vol.* 29, *part* 4, *pp.* 781–821
Printed in Great Britain

On the trapping of wave energy round islands

By M. S. LONGUET-HIGGINS
National Institute of Oceanography, Wormley, Surrey

(Received 28 December 1966)

It is shown that islands can trap long-wave energy in a way similar to the capture of a particle by an atomic nucleus. The frequencies of the captured waves form a discrete set, being determined by the shape of the island and the contours of the surrounding sea bed. If the depth at great distances tends to a constant value, the trapped modes must leak some energy to infinity, though the consequent rate of decay may be exceedingly small. The initial energy of the trapped modes may be absorbed from incident radiation of the same frequency or from a sharp pulse. The particular example of a rectilinear pulse incident on a circular island is discussed in some detail.

The effect of the rotation of the Earth is to split the frequencies of a pair of waves progressing in opposite directions round the island. The splitting of the frequencies produces slow beats in the waves as seen at any fixed point. Slight asymmetry in the island induces a slow exchange of energy between each pair of progressive modes.

The present investigation was suggested by the occurrence of regular oscillations having a period of 6 min and a beat period of about 3 h in long-wave records taken at Macquarie Island, in the Southern Ocean.

Contents

1. Introduction

During a recent visit to the University of Adelaide the author was shown a long-wave record made at Buckles Bay, Macquarie Island (lat. 54° 30′ S, 158° 58′ E) by members of the Department of Mathematics. In this record there appeared a pronounced oscillation of period 6 min lasting for at least 2 days. The amplitude of the oscillations fluctuated with a period of about 3 h.

Macquarie Island is about 22 miles long and is surrounded by a narrow shelf where the depth is a few hundred metres, the whole feature standing out of water of oceanic depth, about 4000 m.

These circumstances led the author to consider whether it was possible for radiation to be trapped round the island by the form of the bottom contours, the characteristic frequency or frequencies being determined by the dimensions of the island.

The first known instance of trapped radiation in hydrodynamics appears to be the 'edge-wave' of Stokes (1846). This is a type of motion possible in the neighbourhood of a plane beach inclined to a constant angle α to the horizontal. The wave progresses parallel to the shoreline, its amplitude diminishing exponentially with distance seawards (measured along the bottom). The frequency σ is connected to the wave-number m parallel to the shoreline by the equation

$$\sigma^2 = gm \sin \alpha, \tag{1.1}$$

where g denotes the acceleration of gravity (see Lamb 1932, p. 260).

Stokes's edge-waves were generalized by Ursell (1952*a*), who showed that it was possible to have higher modes of oscillation in which there were n nodal lines running parallel to the shore, where $n \geqslant 0$.

Much light was thrown on this phenomenon by the work of Eckart (1950, 1951) who considered especially waves whose length was great compared to the local depth of water. He pointed out, in effect, that the trapping of wave energy near the edge of the shoreline was due to the refraction of the waves towards the shore; the speed of propagation of long waves in uniform depth h being equal to $(gh)^{\frac{1}{2}}$, waves in the greater depth of water will be propagated at greater speed, and hence refracted towards the shore.

Ursell (1951) also proved analytically the existence of trapped waves travelling along a submerged circular cylinder. It is now clear that we can consider the cylinder as a wave-guide towards which the waves are refracted by the increasing velocity of propagation on either side.

Some evidence for the generation of edge waves by storms travelling parallel to the continental shelf was presented by Munk, Snodgrass & Carrier (1956), and further theoretical calculations relating to this problem have been carried out by Greenspan (1956), Reid (1958) and Kajiura (1958). In particular Reid (1958) showed that the effect of coriolis forces on an edge-wave travelling parallel to a straight coastline was to increase the velocity of waves travelling in one sense and to decrease the velocity of waves travelling in the opposite sense. More recently Snodgrass, Munk & Miller (1962) have shown the probable existence of edge waves in the spectrum of long waves along the coast of California.

Now in the case of an ideal circular island of sufficiently large radius, it is evident that any small portion of the coast can be regarded as straight locally, and hence we shall expect some waves to be guided round the island by the bottom topography. Moreover, we can predict that for certain wavelengths and frequencies, a trapped wave, after describing one complete circuit, will remain in phase with itself. Hence we expect a discrete set of eigenfrequencies, characteristic of each island. It remains to be seen whether the energy in each mode is completely trapped, or whether some is radiated to infinity. In the latter case the corresponding eigenfrequency should be complex. The question of how such modes may be generated has also to be investigated, and also what is the effect of coriolis forces.

In the present paper we investigate the problem by stages beginning with waves in a uniform depth of water and without coriolis forces; next showing the manner in which waves are trapped along a straight discontinuity, and then proceeding to the case of circular symmetry. It is shown that for a circular 'sill' eigenfrequencies do exist, but if the depth tends to a uniform value at great distances from the centre, then some energy must leak away to infinity. Nevertheless, the rate of decay of some eigenfrequencies is extremely slow, so that the waves are in effect trapped. The situation is somewhat analogous to the slow decay of a resonating bell, which radiates sound to infinity.

In § 8 we investigate the response of the system to a pulse of energy sweeping across the horizontal plane. This corresponds roughly to striking the bell. It is shown that energy can indeed be injected into the trapped modes in this way.

In § 9 we consider how far the results for the circular island may be applied to islands of other shapes, and in § 10 we consider the effect of the rotation of the earth. The rotation is shown to cause a splitting in the frequencies of modes progressing respectively clockwise and anticlockwise round the island. The frequency-splitting in turn produces beats in the wave amplitude.

The conclusions are summarized in §13.

2. The shallow-water equations

Some light can be thrown on the phenomenon of wave trapping by considering the simplest possible case: that of long waves in shallow water.

Let x and y be horizontal Cartesian co-ordinates, and let u, v be the corresponding components of the velocity. Let $\zeta(x, y, t)$ denote the elevation of the free surface above its equilibrium level. Then on the assumption that the vertical acceleration is small compared to g (the acceleration of gravity) it follows that the excess pressure above the hydrostatic pressure equals $\rho g\zeta$, where ρ is the density. Hence the linearized equations of motion may be written

$$\left.\begin{aligned} \frac{\partial u}{\partial t} &= -\frac{\partial}{\partial x}(g\zeta), \\ \frac{\partial v}{\partial t} &= -\frac{\partial}{\partial y}(g\zeta). \end{aligned}\right\} \tag{2.1}$$

Assuming that ζ is small compared to the depth $h(x, y)$ of water in the undisturbed state, we have also the equation of continuity

$$\frac{\partial \zeta}{\partial t} = -\frac{\partial}{\partial x}(hu) - \frac{\partial}{\partial y}(hv). \tag{2.2}$$

On differentiating both sides of (2.2) with respect to t and substituting for u and v from equations (2.1) we have

$$\begin{aligned} \frac{\partial^2 \zeta}{\partial t^2} &= -\frac{\partial}{\partial x}\left(h\frac{\partial u}{\partial t}\right) - \frac{\partial}{\partial y}\left(h\frac{\partial v}{\partial t}\right) \\ &= \frac{\partial}{\partial x}\left(gh\frac{\partial \zeta}{\partial x}\right) + \frac{\partial}{\partial y}\left(gh\frac{\partial \zeta}{\partial y}\right) \\ &= gh\nabla^2\zeta + \nabla(gh).\nabla\zeta, \end{aligned} \tag{2.3}$$

where ∇^2 denotes $\partial^2/\partial x^2 + \partial^2/\partial y^2$. Thus

$$\left(\nabla^2 - \frac{1}{gh}\frac{\partial^2}{\partial t}\right)\zeta + \frac{1}{h}\nabla h.\nabla\zeta = 0. \tag{2.4}$$

At a discontinuity in h we shall assume that

$$\zeta \text{ is continuous} \tag{2.5}$$

and that the normal component of the total flow is continuous, that is

$$h\mathbf{u}.\mathbf{n} \text{ is continuous}, \quad \mathbf{u} = (u, v). \tag{2.6}$$

This assumption has been shown by Bartholomeusz (1958) to give correct results for the reflexion coefficient of long waves incident on a step, even though the vertical acceleration is not small locally. A rigid wall is equivalent to $h = 0$. Hence on both sides of the wall

$$h\mathbf{u}.\mathbf{n} = 0. \tag{2.7}$$

When the motion is simple-harmonic, we may write

$$\zeta \propto e^{-i\sigma t}, \tag{2.8}$$

where σ denotes the radian frequency. Then (2.4) becomes

$$\left(\nabla^2 + \frac{\sigma^2}{gh}\right)\zeta + \frac{1}{h}\nabla h.\nabla\zeta = 0. \tag{2.9}$$

In the special case when the bottom is flat, ∇h vanishes and equation (2.8) reduces to

$$\left(\nabla^2 + \frac{\sigma^2}{gh}\right)\zeta = 0. \tag{2.10}$$

The boundary condition (2.6) becomes

$$h\frac{\partial \zeta}{\partial n} \text{ is continuous.} \tag{2.11}$$

3. The trapping of waves on a straight ledge

The expression $$\zeta = A \exp[i(lx + my - \sigma t)] \tag{3.1}$$
representing a simple harmonic wave of length $L = 2\pi/(l^2+m^2)^{\frac{1}{2}}$ and period $T = 2\pi/\sigma$, satisfies equation (2.10) provided that

$$l^2 + m^2 = \sigma^2/gh. \tag{3.2}$$

Hence the speed of propagation c is given by

$$c = \frac{L}{T} = \frac{\sigma}{(l^2+m^2)^{\frac{1}{2}}} = (gh)^{\frac{1}{2}}, \tag{3.3}$$

by equation (3.2). This is the well-known formula for the speed of propagation of waves in shallow water of depth h.

If in (3.1) we suppose that l, say, is imaginary, then the solution increases exponentially in one horizontal direction, the negative x-direction. The energy to the right of any given line $x =$ constant is finite. However, to exclude infinitely large wave amplitudes as $x \to -\infty$, the left half of the plane must also be excluded. A rigid barrier at $x =$ constant is not sufficient, since the boundary condition there cannot generally be satisfied.

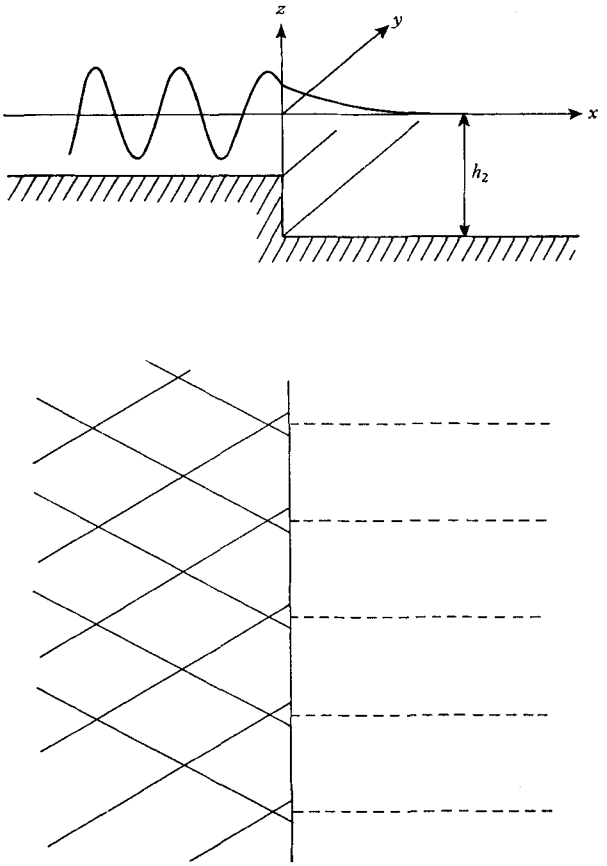

FIGURE 1. Waves near a straight discontinuity in depth. (*a*) Section in a vertical plane; (*b*) the wave crests in plan view.

However, we shall see that with a change in depth along the line $x =$ constant it is possible to have finite energy in the right half-plane.

Suppose then that along the line $x = 0$ there is a discontinuity in the depth, with $h = h_1$ when $x < 0$, and $h = h_2 > h_1$ when $x > 0$, as in figure 1. Let us consider waves which vary harmonically in the y-direction with wave-number m and try

$$\zeta = \exp[i(my - \sigma t)] \times \begin{cases} A\cos l_1 x + B\sin l_1 x & (x < 0), \\ C\,e^{-l_2' x} & (x > 0). \end{cases} \tag{3.4}$$

These expressions satisfy equation (2.10) provided that

$$l_1^2 = \frac{\sigma^2}{gh_1} - m^2, \qquad l_2'^2 = -\frac{\sigma^2}{gh_2} + m^2. \tag{3.5}$$

This is possible† if

$$\frac{\sigma^2}{gh_2} < m^2 < \frac{\sigma^2}{gh_1} \tag{3.6}$$

that is to say

$$\frac{h_1}{h_2} < \frac{m^2 g h_1}{\sigma^2} < 1. \tag{3.7}$$

To satisfy the boundary conditions (2.5) and (2.6) at $x = 0$ we must have $A = C$ and $Bl_1 h_1 = -Cl_2' h_2$ respectively. So writing for convenience $A = l_1 h_1$ we have

$$\zeta = \exp[i(my - \sigma t)] \times \begin{cases} l_1 h_1 \cos l_1 x - l_2' h_2 \sin l_1 x & (x < 0), \\ l_1 h_1\, e^{-l_2' x} & (x > 0). \end{cases} \tag{3.8}$$

The form of the solution is as shown in figure 1*a*: in the shallower depth of water to the left of the discontinuity the solution is sinusoidal; in the deeper water to the right it is exponential. A plan view of the solution is shown in figure 1*b*, the solid lines on the left representing wave crests; and the broken lines on the right the crests of waves decreasing exponentially as x increases.

The solution can also be considered from the point of view of wave refraction, as follows. In the region $x < 0$ the solution (3.8) may be written

$$\zeta = \tfrac{1}{2}R[\exp[i(l_1 x + my - \sigma t + \delta)] + \exp[i(-l_1 x + my - \sigma t - \delta)]], \tag{3.9}$$

where

$$R = (l_1^2 h_1^2 + l_2'^2 h_2^2)^{\frac{1}{2}}, \quad \delta = \tan^{-1}\frac{l_2' h_2}{l_1 h_1}. \tag{3.10}$$

The first term in square brackets in (3.9) represents a wave propagated in the shallow water $h = h_1$ to the left of the discontinuity. The angle of incidence at the discontinuity has a sine equal to $m/(l_1^2 + m^2)^{\frac{1}{2}}$, that is to say $m(gh_1)^{\frac{1}{2}}/\sigma$, by (3.5). The critical angle, on the other hand, has a sine given by c_1/c_2, $= (h_1/h_2)^{\frac{1}{2}}$. We see then from (3.8) that the angle of incidence exceeds the critical angle and hence the waves are totally reflected, the reflected wave being given by the second term in (3.9). On the right of the discontinuity there is only an exponentially decaying 'fringe'. At the barrier itself the wave undergoes a phase-change equal to 2δ.

If now a vertical barrier is placed along the line $x = -a$, forming a 'ledge' of width a and depth h_1 between $x = -a$ and $x = 0$, then we must also satisfy the boundary condition (2.7) at the barrier. We have then

$$\left(\frac{\partial \zeta}{\partial x}\right)_{x=-a} = 0, \tag{3.11}$$

† Without loss of generality we may assume l_1 and l_2', if real, to be positive.

or $$Rl_1 \exp[i(my - \sigma t)] \sin(l_1 a - \delta) = 0. \tag{3.12}$$

Hence $$l_1 a = \delta + n\pi, \tag{3.13}$$

where n is an integer. Regarded in another way, the condition (3.11) is equivalent to specifying that the phases of the incident and reflected waves at the barrier are equal. Hence the total phase-change in crossing and recrossing the shelf normally (y and t held constant) is $(2l_1 a - 2\delta)$ and this must be equal to $2n\pi$. From (3.13) we have

$$\tan(l_1 a) = \tan\delta = \frac{l_2' h}{l_1 h}. \tag{3.14}$$

From (3.5) we have $$l_2'^2 = (1 - h_1/h_2) m^2 - (h_1/h_2) l_1^2. \tag{3.15}$$

So on substituting in (3.14) we find

$$(l_1 a) \tan(l_1 a) = \sqrt{[(h_2/h_1)(h_2/h_1 - 1)(ma)^2 - (h_2/h_1)(l_1 a)^2]}. \tag{3.16}$$

Under the conditions of our problem $h_2/h_1 > 1$, so that for given non-zero values of m and a the above equation has a discrete set of solutions. Thus for a shelf of given width a and for a given wavelength $2\pi/m$ along the shelf there exists a discrete set of modes in which the energy is trapped over the shelf. The corresponding wave frequencies are found from the relation

$$\frac{\sigma^2 a^2}{g h_1} = (l_1 a)^2 + (ma)^2. \tag{3.17}$$

On squaring both sides of (3.16) we obtain the relation

$$(l_1 a)^2 [\tan^2(l_1 a) + (h_2/h_1)] = (ma)^2 (h_2/h_1)(h_2/h_1 - 1), \tag{3.18}$$

which is equivalent to equation (3) of Snodgrass *et al.* (1962). These authors have computed the frequencies corresponding to real values of the wave-number l_1. We may note in passing that the equation (3.18), since it is derived from squaring (3.13) contains also solutions corresponding to the situation when l_2' is negative. These represent waves whose amplitude increases exponentially with distance from the shelf. Hence they do not correspond to trapped waves.

We note that (3.18) can also be written

$$\sec^2 z + P - \frac{Q}{z^2} = 0, \tag{3.19}$$

where

$$\left.\begin{aligned} z &= l_1 a, \\ P &= \frac{h_1}{h_2} - 1, \\ Q &= P(P+1)(ma)^2. \end{aligned}\right\} \tag{3.20}$$

It can be shown that besides the real solutions to this equation there exist also solutions with z complex and $\mathscr{R}(l_2') < 0$. These represent waves whose amplitude is a function of x both over the shelf ($x < 0$) as well as in the deeper water. Their

frequency is complex and their energy increases or decays exponentially† with the time t. Later it will be seen that analogous modes occur also in the solution of the period equation for a circular island (see § 6).

4. Parallel bottom contours: the general case

Consider now the general case in two dimensions when the mean depth h is a function of x only. The contours of h = constant are then straight and parallel to the y-axis.

The differential equation (2.9) reduces to

$$\left(\nabla^2+\frac{\sigma^2}{gh}\right)\zeta+\frac{h'}{h}\frac{\partial\zeta}{\partial x}=0, \tag{4.1}$$

where a prime denotes differentiation with respect to x. Let us consider waves which are simple-harmonic in the y-direction with constant wave-number m. Then we have

$$\zeta = X(x)\exp\left[i(my-\sigma t)\right] \tag{4.2}$$

and substitution in (4.1) gives

$$X''+\frac{h'}{h}X+\left(\frac{\sigma^2}{gh}-m^2\right)X=0. \tag{4.3}$$

which can also be written

$$(hX')'+\left(\frac{\sigma^2}{gh}-m^2h\right)X=0. \tag{4.4}$$

The behaviour of $X(x)$ depends upon the sign of the final term. For writing $hX' = Y$ we have

$$\left.\begin{aligned} X' &= (1/h)\,Y, \\ Y' &= -(\sigma^2/g-m^2h). \end{aligned}\right\} \tag{4.5}$$

If $(\sigma^2/g-m^2h) > \delta > 0$ then by plotting X and Y as functions of x it is easy to see that the point (X, Y) describes a path enclosing the origin, that is, X and Y are oscillatory functions of x. On the other hand if $(\sigma^2/g-m^2h) < \delta < 0$ as x tends to infinity, then X and Y both tend to infinity or both tend to zero as $x \to \infty$.

Since we are considering shallow water ($h \ll L$), we are not free to assume that $h \to \infty$ as $x \to \infty$. However, we may suppose that h tends to a finite value h_∞, say. Then the behaviour of X is sinusoidal or exponential at infinity according as $h_\infty \gtrless \sigma^2/gm^2$. In order that the waves shall have finite energy over the range $(0, \infty)$ it is necessary that $h_\infty \geqslant \sigma^2/gm^2$ and that we choose the solution X tending to 0 as $x \to \infty$. If $h \to h_\infty$ as $x \to \infty$, and $h \to h_{-\infty}$ as $h \to -\infty$ then in general we have an eigenvalue problem to solve for X.

If on the other hand $h_\infty < \sigma^2/gm^2$ then either the total energy is infinite or else there is a slow leak of energy to and from infinity in the x-direction.

† These modes are not discussed by Snodgrass *et al.* (1962) who are concerned only with real values of σ. Budden (1961) calls such decaying modes 'leaky'. Snodgrass *et al.* use the same term in a different sense.

It is clear that for any given value of h_∞, there will always be frequencies σ and wave-numbers m such that $h_\infty > \sigma^2/gm$. Hence on a straight coastline we expect that there will always be some modes which are trapped at the shoreline. The contrast with the circular shoreline will now become apparent.

5. Circular bottom contours

Let r and θ be polar co-ordinates in the horizontal plane, and suppose that h is a function of r only. The bottom contours are then circles centred on the origin. The differential equation (2.10) reduces to

$$\left(\nabla^2 + \frac{\sigma^2}{gh}\right)\zeta + \frac{h'}{h}\frac{\partial \zeta}{\partial r} = 0, \tag{5.1}$$

where

$$\nabla^2 = \frac{1}{r^2}\left[\left(r\frac{\partial}{\partial r}\right)^2 + \frac{\partial^2}{\partial \theta^2}\right], \tag{5.2}$$

and a prime denotes differentiation with respect to r. Let us suppose also that $\zeta \propto e^{in\theta}$ where n is an integer, that is

$$\zeta = R(r)\exp\left[i(n\theta - \sigma t)\right]. \tag{5.3}$$

Then on substituting in (5.1) we have

$$R'' + \left(\frac{1}{r} + \frac{h'}{h}\right)R' + \left(\frac{\sigma^2}{gh} - \frac{n^2}{r^2}\right)R = 0, \tag{5.4}$$

which can also be written

$$(hrR')' + \left(\frac{\sigma^2}{g} - \frac{n^2 h}{r^2}\right)rR = 0. \tag{5.5}$$

If we let $hrR' = S$ then we have

$$\left.\begin{aligned} R' &= \frac{1}{hr}S \\ \text{and from (5.5)} \qquad S' &= -\left(\sigma^2/g - n^2h/r^2\right)R. \end{aligned}\right\} \tag{5.6}$$

A similar argument then shows that R is oscillatory or exponential according as

$$\sigma^2/g \gtrless n^2h/r^2. \tag{5.7}$$

Now if we suppose that as $r \to \infty$ then the depth h tends to a constant value h_∞; the right-hand side of (5.7) must tend to 0 and so ultimately σ^2/g exceeds n^2h/r^2. Hence under these conditions the solution is oscillatory at great distances, and trapped waves are impossible, with circular symmetry. We shall see, however, that if the wave-number is sufficiently large, then the loss of energy to infinity can be made exceedingly small.

The physical reason for the impossibility of perfect trapping is as follows. The waves tend always to be propagated with the local velocity $(gh)^{\frac{1}{2}}$. With circular symmetry, the average *angular* velocity of the waves about the centre is then $(gh)^{\frac{1}{2}}/r$. In order that the wave energy shall be refracted inwards, this velocity must increase, or at least not decrease, as r increases, that is to say

$$\frac{d}{dr}\frac{(gh)^{\frac{1}{2}}}{r} \geqslant 0. \tag{5.8}$$

This implies that
$$\frac{(gh)^{\frac{1}{2}}}{r} \geqslant \text{constant}; \quad h \geqslant \text{constant} \times r^2. \tag{5.9}$$

That is, h must increase at least like r^2 for trapping to be possible.

Generally, if at some distance from the centre $(\sigma^2/g - n^2h/r^2)$ is negative, it must change sign at a critical radius r_0 say. This will be given by
$$r_0^2 = \frac{n^2gh}{\sigma^2} = \frac{n^2c^2}{\sigma^2}, \tag{5.10}$$

where $c = (gh)^{\frac{1}{2}}$ is the local velocity of propagation of free waves.

The foregoing conclusions are illustrated by the particular case when the depth h is everywhere uniform. Then (5.4) becomes
$$R'' + \tfrac{1}{2}R' + \left(\frac{\sigma^2}{gh} - \frac{n^2}{r^2}\right) R = 0 \tag{5.11}$$

of which the general solution is
$$R = AJ_n(kr) + BY_n(kr) \tag{5.12}$$

where
$$k = \frac{\sigma}{(gh)^{\frac{1}{2}}}. \tag{5.13}$$

Now J_n and Y_n have the following asymptotic forms for large n (see Jeffreys & Jeffreys 1950, § 21.06). When $\xi > n$,
$$\left.\begin{aligned} J_n(\xi) &\sim \left(\frac{2}{n\pi \tan u}\right)^{\frac{1}{2}} \cos\left[n(\tan u - u) - \tfrac{1}{4}\pi\right], \\ Y_n(\xi) &\sim \left(\frac{2}{n\pi \tan u}\right)^{\frac{1}{2}} \sin\left[n(\tan u - u) - \tfrac{1}{4}\pi\right], \\ u &= \cos^{-1}(n/\xi); \end{aligned}\right\} \tag{5.14}$$

and when $\xi < n$,
$$\left.\begin{aligned} J_n(\xi) &\sim \left(\frac{1}{2n\pi \tanh v}\right)^{\frac{1}{2}} \exp\left[-n(v - \tanh v)\right], \\ Y_n(\xi) &\sim -\left(\frac{2}{n\pi \tanh v}\right)^{\frac{1}{2}} \exp\left[n(v - \tanh v)\right], \\ z &= \cosh^{-1}(n/\xi), \end{aligned}\right\} \tag{5.15}$$

(see also Watson 1922 § 8.4)†. Thus when $\xi < n$ the solutions are exponential, and when $\xi > n$ they are sinusoidal. The transition comes when
$$kr = \xi = n \tag{5.16}$$

that is to say
$$r = \frac{n}{k} = \frac{n(gh)^{\frac{1}{2}}}{\sigma}, \tag{5.17}$$

which is the turning point given by (5.10).

It follows that the solution
$$\zeta = J_n(kr) \exp\left[i(n\theta - \sigma t)\right] \tag{5.18}$$

† These formulae, generally attributed to Debye (1909), were first obtained by L. V. Lorenz (1890). For further terms see Bickley (1943).

can be interpreted in the following way (see figure 2). In the region $kr > n$ the solution is wave-like and equation (5.14) shows that the wave-number in the radial direction is given by

$$\begin{aligned} & n\frac{d}{dr}(\tan u - u), \\ &= n(\sec^2 u - 1)\frac{du}{dr}, \\ &= n\tan^2 u \frac{du}{d\xi}\frac{d\xi}{dr}, \\ &= n\tan^2 u \operatorname{cosec} u \frac{u}{\xi^2} k, \\ &= k\sin u, \\ &= (k^2 - n^2/r^2)^{\frac{1}{2}}. \end{aligned} \tag{5.19}$$

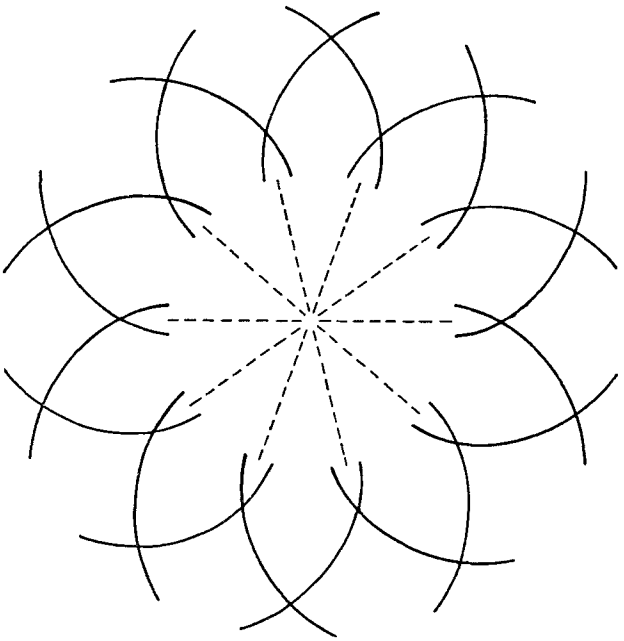

FIGURE 2. The form of the function $J_n(kr)\, e^{in\theta}$ when $n = 10$.

The wave-number in the transverse direction is n/r. Hence the total wave-number is

$$k = \frac{\sigma}{(gh)^{\frac{1}{2}}}, \tag{5.20}$$

which is a constant. Hence the wave-length of the waves is a constant, and the waves are propagated locally with the free-wave velocity $(gh)^{\frac{1}{2}}$. Moreover, the angle between the local wave-number and the radius vector is equal to $(\frac{1}{2}\pi - u)$, which shows that the perpendicular from the origin to the ray-path has a length $r\cos u$ equal to n/k. Hence the ray-paths are straight lines tangent to the critical circle $r = n/k$. Incidentally this provides us with an asymptotic method of constructing the phase lines of the Bessel function solution (5.20): draw the tangents to the fixed circle $r = n/k$, and then construct the ray orthogonals.

A precisely similar description applies to the behaviour of the second solution $\zeta \propto Y_n(kr)\exp[i(n\theta-\sigma t)]$ outside the critical circle, except that the waves represented by the latter are in quadrature with those represented by the first solution.

The pattern of crests of $J_n(kr)\,e^{in\theta}$ is shown in figure 2. Outside the critical radius $r = n/k$ the waves have the form of spirals so arranged that the local wavelength is everywhere constant. At large distances the crests are almost transverse. As r diminishes they must turn and become more radial, in order to maintain the same number n of oscillations round the circumference of each circle. At the critical radius their crests are radial and then can turn no more. When $r < n/k$ the wave-number in the radial direction become imaginary and the waves increase or decrease exponentially inwards; J_n decreases exponentially, and Y_n increases exponentially as r diminishes. In fact Y_n, as is well known, has a logarithmic singularity at $r = 0$, but this is over-shadowed by the factor r^{-n} which represents an almost exponential increase as $r \to 0$.

In the sinusoidal region $r > n/k$, the asymptotic expressions (5.16) show that the amplitude of the oscillation is proportional to $(\tan u)^{-\frac{1}{2}}$ and hence to $r^{-\frac{1}{2}}$ as $r \to \infty$. So the energy density falls off as r^{-1}, and the energy per unit distance r from the centre is a constant. The total energy of the disturbance is infinite. In this sense the energy is not trapped.†

In the neighbourhood of the critical radius neither of the asymptotic expansions (5.16) or (5.17) is applicable. However, in that case it may be shown that J_n and Y_n are described asymptotically by Airy functions (see Olver 1954).

An analogous interpretation may be given of the Hankel function solution

$$\zeta = H_n^{(1)}(kr)\exp[i(n\theta-\sigma t)] \tag{5.21}$$

and similarly of the solution with $H_n^{(2)}$, where

$$\left.\begin{aligned} H_n^{(1)} &= J_n - iY_n, \\ H_n^{(2)} &= J_n + iY_n. \end{aligned}\right\} \tag{5.22}$$

The asymptotic expansions (5.14) show that for large values of ξ greater than n

$$H_n^{(1)}(\xi) \sim \left(\frac{2}{n\pi\tan u}\right)^{\frac{1}{2}} \exp\{i[n(\tan u - u) - \tfrac{1}{4}\pi]\}, \tag{5.23}$$

and so the solution (5.23) is given by

$$\zeta \sim \left(\frac{2}{n\pi\tan u}\right)^{\frac{1}{2}} \exp\{i[n(\tan u - u) + n\theta - \sigma t - \tfrac{1}{4}\pi]\}, \tag{5.24}$$

where $u = \arccos(n/kr)$. This represents a wave rotating about the origin in the positive (anticlockwise) direction, and with the arms spiralling outwards to infinity. There is clearly a net flux of energy radially outwards, given by the time-mean of $\rho g\zeta^2 . 2\pi r \sin u . c$, that is to say

$$F = 4\rho g^2 h/\sigma. \tag{5.25}$$

Such a wave is possible physically only if there is a source of energy at the origin. Since $J_n = \frac{1}{2}(H_n^{(1)} + H_n^{(2)})$ the first solution discussed above, namely (5.18) may be regarded as the sum of two solutions, in one of which the energy is spiralling

† This sense of 'trapping' appears to be more in accordance with normal usage than that suggested by Chambers (1965).

outwards, and the other in which it is spiralling inwards, the radial components of the two fluxes being equal and opposite. The tangential components of the flux are in the same (anticlockwise) sense and reinforce one another. We may note that since motions proportional to J_n and Y_n require a source and sink of energy at infinity in order to maintain them, they cannot be said to represent trapped wave motions.

An important property of the Hankel function solution (5.22) is that *inside* the critical circle it tends to be dominated by the term involving Y_n, which as we saw increases exponentially towards the centre. Hence $H_n^{(1)}$, regarded in the opposite way, decreases almost exponentially as one travels outwards within this region. The above property is very relevant to the following discussion.

6. Free waves round a circular sill

To represent a circular sill or sea-mount of radius a, let us suppose that the mean depth of water is given by $h = h_1$ when $0 \leqslant r < a$ and $h = h^2$ when $r > a$ (see figure 3*a*). Since ζ is to be finite at $r = 0$ the second solution Y_n is excluded when $r < a$. Let us then try

$$\zeta = \exp[i(n\theta - \sigma t)] \times \begin{cases} AJ_n(k_1 r) & (0 \leqslant r < a) \\ BH_n^{(1)}(k_2 r) & (r > a) \end{cases} \tag{6.1}$$

where A and B are constants and where

$$k_1 = \frac{\sigma}{(gh_1)^{\frac{1}{2}}}, \qquad k_2 = \frac{\sigma}{(gh_2)^{\frac{1}{2}}}. \tag{6.2}$$

The solution is illustrated in figure 3*b*. Inside the sill (that is when $r < a$) the solution consists of two systems of waves propagated along straight trajectories tangent to the circle $k_1 r = n$. This circle we may call the inner critical circle. Outside the sill the solution consists of waves propagated outwards, along straight trajectories all tangent to the circle $k_2 r = n$ (the outer critical circle). Hence there is necessarily some loss of energy to infinity. However, if the distance between the outer critical circle and the edge of the sill is more than a wave-length $2\pi/k_2$ then because of the exponential decrease of $H_n^{(1)}$ noted above, the amplitude of the waves at the outer critical circle is exponentially small compared to the amplitude at the edge of the sill. Hence the loss of energy to infinity in one wave period will be very small compared to the total energy contained over the sill. The waves are then practically, but not absolutely, trapped.

From the above discussion it appears that two necessary conditions for the existence of trapped modes are, first, that the ray paths in the interior must make with the normal at the sill an angle greater than the critical angle. Hence

$$\frac{n}{k_1 a} > \frac{h_1}{h_2}, \qquad n > \frac{h_1}{h_2}(k_1 a). \tag{6.3}$$

Secondly, the outer critical circle must be sufficiently far from the edge of the sill. Thus

$$k_2(n/k_2 - a) \gg 1, \qquad n \gg 1 + (k_2 a). \tag{6.4}$$

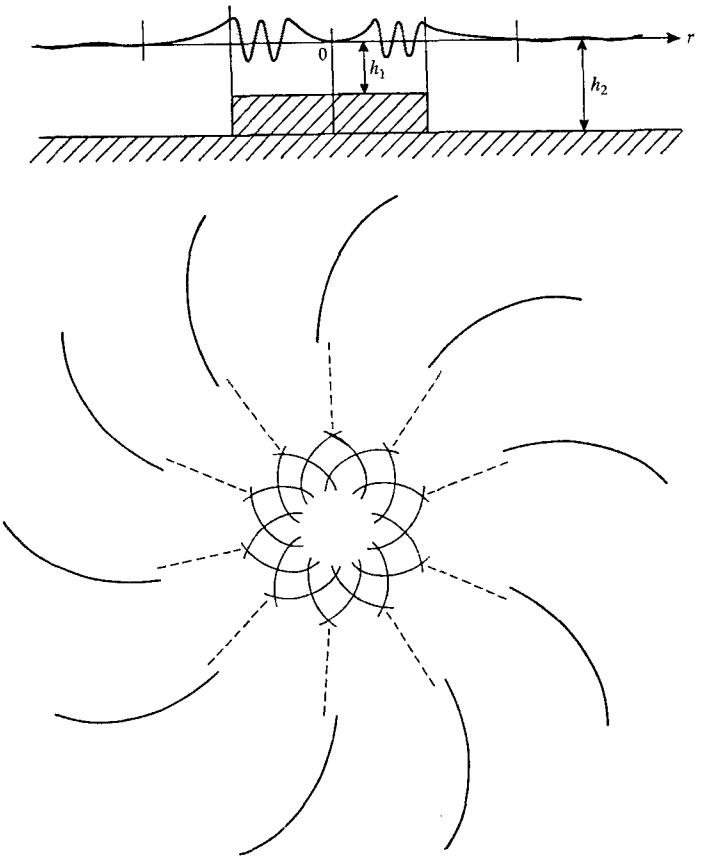

FIGURE 3. The form of free waves trapped by a circular sill. (*a*) A radial cross-section; (*b*) plan view of the wave crests.

Since $k_1/k_2 = (h_2/h_1)^{\frac{1}{2}}$ it appears that the first condition (6.3) is equivalent to $n > (h_1/h_2)^{\frac{1}{2}}(k_2 a)$, so that if the second equation (6.4) is satisfied so also is (6.3).

The above arguments also supply us with an approximate estimate of the frequencies of the trapped modes. For from (5.24) the phase-change after crossing from the edge of the sill to the inner critical radius and back again (keeping θ and t constant) is given by

$$2[n(\tan u - u) - \tfrac{1}{4}\pi], \qquad \cos u = \frac{n}{k_1 a}. \tag{6.5}$$

The constant phase-shift $\frac{1}{2}\pi$ is typically associated with a wave caustic such as the inner critical circle. The above phase must be equal (mod 2π) to the phase shift at the boundary. Approximating the boundary by a straight edge as in § 3, we see that this phase shift is given by

$$2\tan^{-1}\frac{l_2' h_2}{l_1 h_1}, \tag{6.6}$$

where l_1 and l_2' are given by the same formulae (3.5) as before. Here m denotes the wave-number along the edge of the sill, that is to say

$$m = n/a, \quad am = n. \tag{6.7}$$

Hence also
$$l_1 a = (k_1^2 - m^2)^{\frac{1}{2}} a = n \tan u \tag{6.8}$$

and from (3.14)
$$l_2' a = n\sqrt{[1 - (h_1/h_2)\sec^2 u]}. \tag{6.9}$$

So on equating the phases in (6.5) and (6.6) and taking the tangent of half each angle we obtain

$$\tan[n(\tan u - u) - \tfrac{1}{4}\pi] = \sqrt{[(h_2/h_1)\{(h_2/h_1 - 1)\cot^2 u - 1\}]}. \tag{6.10}$$

Given h_2/h_1 and n, this equation may be solved for u. A graphical solution when $n = 4$ and $h_1/h_2 = \frac{1}{16}$, $\frac{1}{4}$ and $\frac{9}{16}$ is shown in figure 4. The corresponding non-dimensional frequencies may be defined by

$$\xi = \frac{a\sigma}{(gh_1)^{\frac{1}{2}}} = ak_1 = n \sec u. \tag{6.11}$$

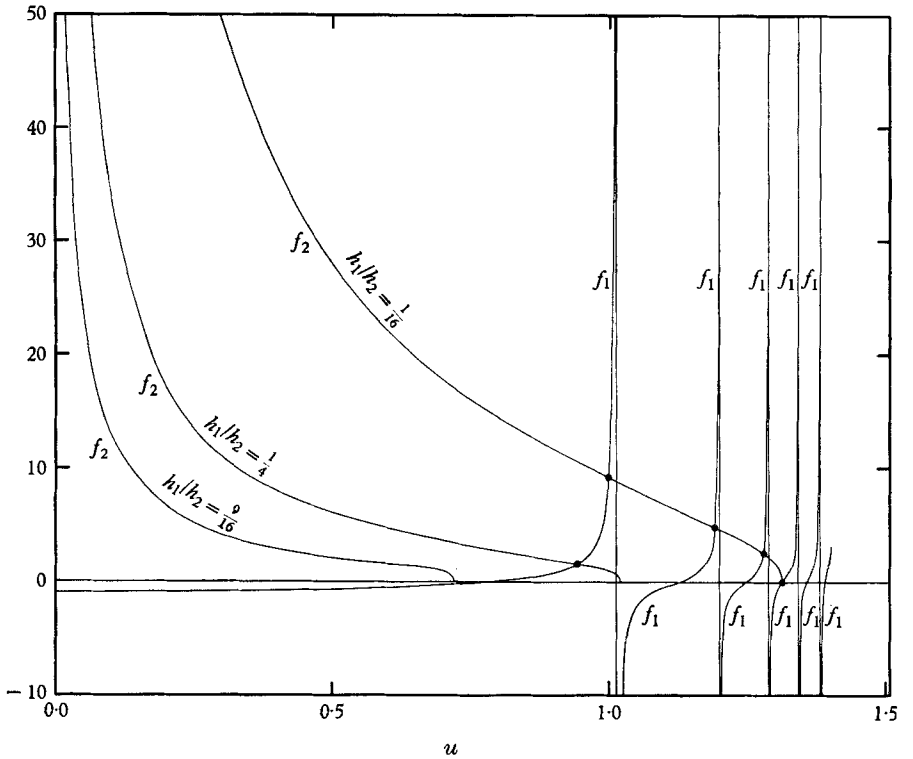

FIGURE 4. Graphs of the functions

$$f_1(u) = \tan[n(\tan u - u) - \tfrac{1}{4}\pi],$$
$$f_2(u) = \sqrt{[(h_2/h_1)\{(h_2/h_1 - 1)\cot^2 u - 1\}]},$$

when $n = 4$ and $h_1/h_2 = \frac{1}{16}$, $\frac{1}{4}$ and $\frac{9}{16}$.

The numerical values of ξ for $n = 1$ to 8 and with the same three values of h_1/h_2 are given in table 1.

	$n =$							
h_1/h_2	1	2	3	4	5	6	7	8
$\frac{1}{16}$	3·408	4·909	6·196	7·423	8·617	9·789	10·944	12·086
	—	7·683	9·436	10·823	12·134	13·407	14·653	15·880
	—	—	11·898	13·942	15·396	16·754	18·069	19·356
	—	—	—	16·000	18·433	19·954	21·347	22·691
	—	—	—	—	—	22·901	24·502	25·927
	—	—	—	—	—	—	27·332	29·042
$\frac{1}{4}$	—	3·897	5·474	6·843	8·114	9·333	10·521	11·686
	—	—	—	—	—	11·972	13·597	15·022
$\frac{9}{16}$	—	—	—	—	6·667	7·986	9·247	10·484

TABLE 1. Approximate frequencies of trapped modes of oscillation, from equation (6.10): values of $\xi = a\sigma/(gh_1)^{\frac{1}{2}}$

To obtain accurate values of the frequencies and rates of damping we return to the solution (6.1) and apply the boundary conditions (2.5) and (2.6) at the edge of the sill ($r = a$). We have then to satisfy the two equations

$$\left.\begin{aligned} AJ_n(k_1 a) &= BH_n(k_2 a), \\ Ak_1 h_1 J_n'(k_1 a) &= Bk_2 h_2 H_n'(k_2 a), \end{aligned}\right\} \tag{6.12}$$

where we have written H_n for $H_n^{(1)}$ and a prime denotes differentiation with respect to the argument. For brevity write

$$k_1 a = \frac{\sigma a}{(gh_1)^{\frac{1}{2}}} = z = \xi - i\eta, \tag{6.13}$$

representing a dimensionless frequency, and also

$$k_2/k_1 = (h_1/h_2)^{\frac{1}{2}} = \epsilon, \tag{6.14}$$

a constant parameter. Then equations (6.12) may be written in matrix form

$$\begin{pmatrix} J_n(z) & H_n(\epsilon z) \\ \epsilon J_n'(z) & H_n'(\epsilon z) \end{pmatrix} \begin{pmatrix} A \\ B \end{pmatrix} = \begin{pmatrix} 0 \\ 0 \end{pmatrix}. \tag{6.15}$$

In order that a solution exist the determinant of the matrix must vanish and so z must be a zero of the function

$$F(z) \equiv J_n(z) H_n'(\epsilon z) - \epsilon J_n'(z) H_n(\epsilon z). \tag{6.16}$$

We know that the roots of this equation cannot be real, for the following reason. We have seen that there must be a slow leak of energy to infinity; hence the modes must decay in time, and σ and likewise z must have a small imaginary part (so that $\eta > 0$). We have then to search for the zeros of $F(z)$ in the lower half-plane.

We shall take the cut in the complex plane associated with the function $H_n(\epsilon z)$ to be along the negative imaginary axis. Then the zeros in the left half-plane are simply the reflexion of those in the right half-plane. Hence it is sufficient to find the zeros of $F(z)$ in the lower right half-plane (the fourth quadrant).

The function $F(z)$ has no singularities in the finite part of the plane except at the origin, where it behaves asymptotically like z^{-1}. Thus it is slightly more convenient to deal with the function

$$G(z) \equiv z F(z), \tag{6.17}$$

which is finite but not zero near the origin.†

We may expect (complex) zeros in the neighbourhood of the real values which have already been estimated in table 1. But apart from the zeros representing trapped modes it can be seen that there must also be an infinite sequence of zeros representing modes which decay rapidly with time. These are modes which are wavelike both inside and immediately outside the sill. Analytically, if we adopt the asymptotic formulae of § 5, we see that for sufficiently large values of ξ

$$G(z) \sim \frac{2}{\pi\epsilon^{\frac{1}{2}}} [\epsilon \sin(z-\beta) + i\cos(z-\beta)] \exp[i(\epsilon z - \beta)], \tag{6.18}$$

where β denotes $(\frac{1}{2}n+\frac{1}{4})\pi$. The exponential factor cannot vanish. And since $0 < \epsilon < 1$ it is easy to see that the vanishing of the right-hand side implies that

$$\xi = (\tfrac{1}{2}n + \tfrac{1}{4} + m)\pi, \quad \tanh\eta = \epsilon, \tag{6.19}$$

where m is an integer. This represents a sequence of zeros along the line

$$\eta = \tanh^{-1}\epsilon$$

below and parallel to the real axis, and spaced at intervals of π. Note that when $\epsilon = \frac{1}{4}$, $\frac{1}{2}$ and $\frac{3}{4}$ we have $\tanh^{-1}\epsilon = 0{\cdot}255$, $0{\cdot}549$ and $0{\cdot}973$ respectively.

Starting with the approximate values of z given in table 1 and equation (6.19), the corresponding roots of $G(z)$ were determined numerically by means of successive approximations z_k $(k = 1, 2, 3, \ldots)$ where z_1 denotes the first approximation to any given root and

$$z_{k+1} = z_k - G(z_k)/G'(z_k). \tag{6.20}$$

Convergence was generally rapid. A typical set of results, for $h_1/h_2 = \epsilon^2 = \frac{1}{16}$, can be seen in figure 5*a*. The zeros corresponding to a particular value of n have been joined by a full curve. When $n = 6$, for example, we find a sequence of zeros which for low values of the frequency, lie extremely close to the real axis (the vertical scale is exaggerated relative to the horizontal scale). These zeros represent the modes which are virtually trapped by the circular sill. Following the sequence of zeros in figure 5*a* to the right (ξ increasing) we find that the zeros leave the neighbourhood of the real axis and tend ultimately to the values given by (6.19). The transition from the trapped modes to the damped modes takes place between $\xi = n$ and $\xi = n/\epsilon$.

The accurate values of the zeros $z = \xi - i\eta$ corresponding to the trapped, or almost trapped modes, are given in table 2. Comparison with table 1 will show that the real parts ξ of the frequencies agree quite well with the asymptotic approximation even when the damping, represented by η, is appreciable.

† There is however a cut through the origin. We take this to be from 0 to $-i\infty$ along the negative imaginary axis.

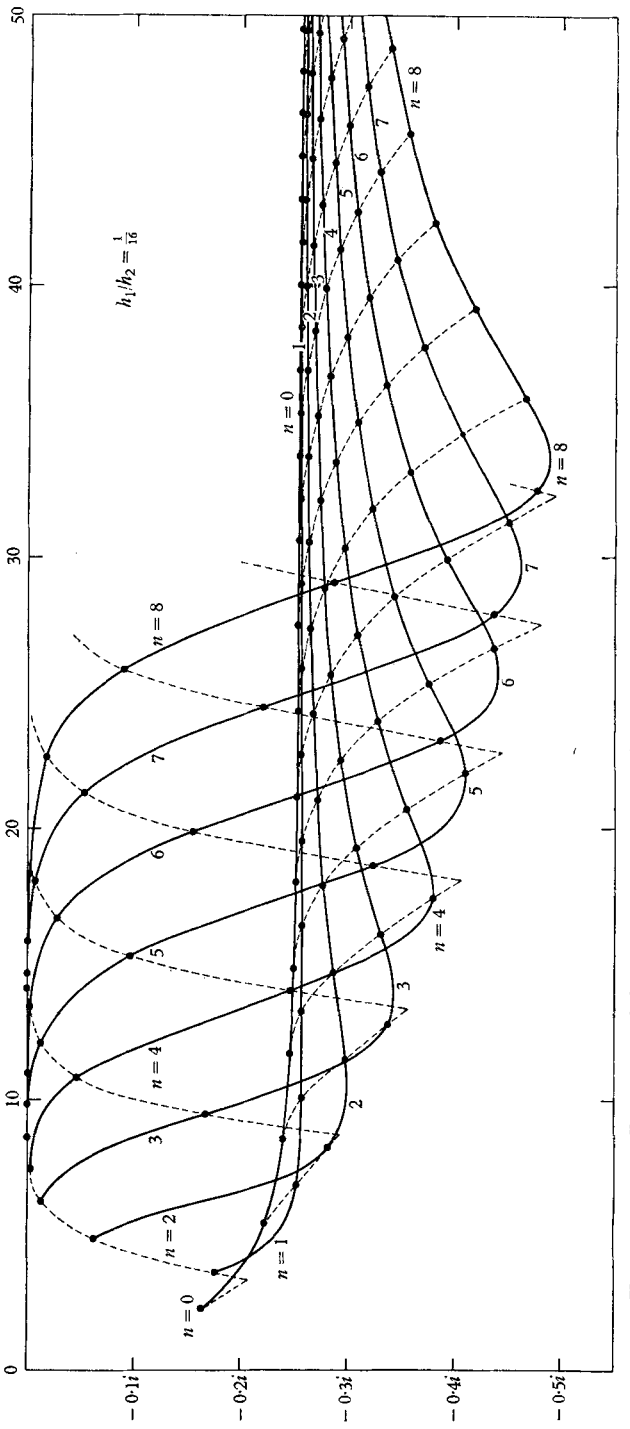

FIGURE 5 (*a*). The zeros of $G(z)$ in the fourth quadrant of the z-plane, when $h_1/h_2 = \frac{1}{16}$; the main sequence.

However, η may in some cases be extremly small, as was predicted. When $h_1/h_2 = \epsilon^2 = \frac{1}{16}$ and $n \geqslant 4$, the damping of the waves, as given by the ratio η/ξ, is of order 10^{-3} or less.

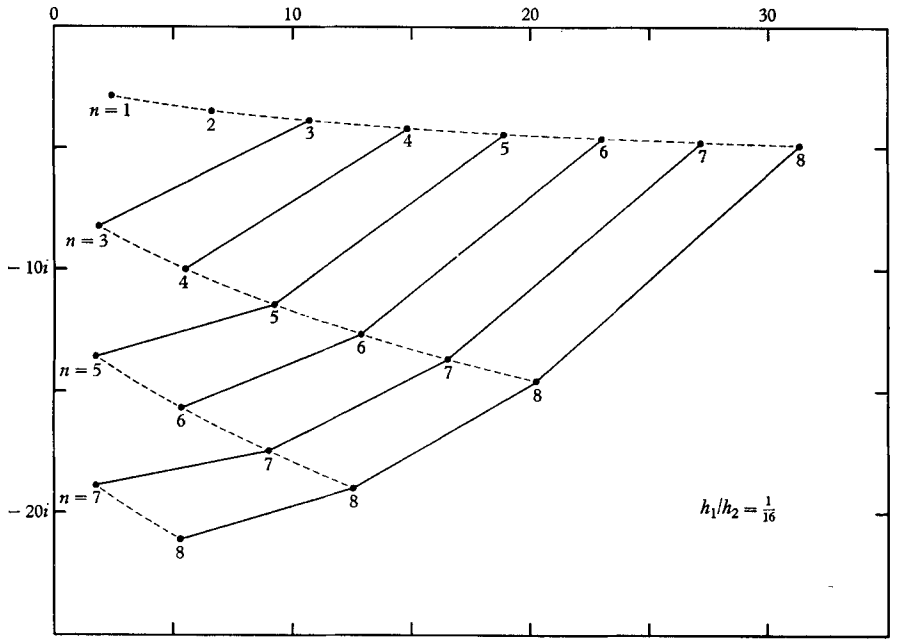

FIGURE 5 (*b*). The zeros of $G(z)$ in the fourth quadrant of the z-plane, when $h_1/h_2 = \frac{1}{16}$: the remaining zeros.

The inner and outer critical radii are also shown in table 2, from which it can be seen that the damping is least (that is the trapping is most effective) when the outer critical radius is appreciably larger than a, that is to say when the condition (6.4) is satisfied. As we saw, this is because of the exponential decrease of the solution between the edge of the sill and the outer critical circle.

In figure 5*a* the first, or left-hand, zero of each of the sequences corresponding to given values of n, has been joined to the others by a broken curve. Similarly, the second zeros are joined by another broken curve, and so on.

In order to see whether all possible zeros of $G(z)$ had been found by the procedure just described, a check was made of the number of zeros of $G(z)$ lying within the square ($0 < \xi < 50$, $0 < \eta < 50$) by means of Rouché's theorem

$$\mathrm{var}_\Gamma(\arg G(z)) = 2\pi(Z-P). \tag{6.21}$$

Here the left-hand side represents the variation of the argument of $G(z)$ round the boundary Γ of the square, and Z and P denote the number of zeros and poles respectively contained within the contour. Since there are no poles within Γ, we have $P = 0$. So by computing the left-hand side we deduce Z.

It turned out that several zeros had not been accounted for. By a systematic search of the area the others were then found. They are shown in figure 5*b* (for $h_1/h_2 = \frac{1}{16}$). In this figure the vertical and horizontal scales are equal, so that the

n	Frequency ξ	Damping η	Critical radii n/ξ	Critical radii $n/(\epsilon\xi)$	D	$\frac{D}{\epsilon\eta}$	$\frac{D}{\epsilon(\xi\eta)^{\frac{1}{2}}}$
			(a) $\epsilon = 0{\cdot}25$				
1	3·656	0·1756	0·27	1·09	0·4363	9·938	2·178
2	4·921	$0{\cdot}6309 \times 10^{-1}$	0·41	1·63	0·2560	16·23	1·838
	8·219	0·2774	0·24	0·97	0·5588	8·057	1·480
3	6·209	$0{\cdot}1246 \times 10^{-1}$	0·48	1·93	0·1158	37·17	1·665
	9·456	0·1566	0·32	1·27	0·4109	10·50	1·351
	12·818	0·3383	0·23	0·94	0·6194	7·324	1·190
4	7·447	$0{\cdot}2172 \times 10^{-2}$	0·54	2·15	0·04962	91·37	1·560
	10·798	$0{\cdot}4613 \times 10^{-1}$	0·37	1·48	0·2180	18·90	1·235
	14·027	0·2462	0·29	1·14	0·5289	8·593	1·138
	17·426	0·3798	0·23	0·92	0·6563	6·913	1·021
5	8·646	$0{\cdot}3613 \times 10^{-3}$	0·58	2·31	0·02066	228·8	1·479
	12·125	$0{\cdot}1091 \times 10^{-1}$	0·41	1·65	0·1073	39·37	1·181
	15·358	$0{\cdot}9563 \times 10^{-1}$	0·33	1·30	0·3142	13·14	1·037
	18·624	0·3237	0·27	1·07	0·6202	7·665	1·010
6	9·821	$0{\cdot}5798 \times 10^{-4}$	0·61	2·44	0·008424	581·1	1·412
	13·408	$0{\cdot}2362 \times 10^{-2}$	0·45	1·79	0·05068	85·81	1·139
	16·723	$0{\cdot}2815 \times 10^{-1}$	0·36	1·44	0·1703	24·21	0·993
	19·922	0·1553	0·30	1·20	0·4046	10·42	0·920
	23·235	0·3870	0·26	1·03	0·6891	7·122	0·919
7	10·978	$0{\cdot}9019 \times 10^{-5}$	0·64	2·55	0·003374	1496	1·356
	14·661	$0{\cdot}4843 \times 10^{-3}$	0·48	1·91	0·02322	191·8	1·102
	18·055	$0{\cdot}7339 \times 10^{-2}$	0·39	1·55	0·08791	47·92	0·966
	21·299	$0{\cdot}5441 \times 10^{-1}$	0·33	1·31	0·2358	17·34	0·876
	24·496	0·2201	0·29	1·14	0·4895	8·896	0·843
	27·856	0·4370	0·25	1·00	0·7392	6·765	0·847
8	12·121	$0{\cdot}1368 \times 10^{-5}$	0·66	2·64	0·001332	3895	1·308
	15·890	$0{\cdot}9485 \times 10^{-4}$	0·50	2·01	0·01038	437·8	1·070
	19·352	$0{\cdot}1785 \times 10^{-2}$	0·41	1·65	0·04379	98·12	0·942
	22·662	$0{\cdot}1642 \times 10^{-1}$	0·35	1·41	0·1304	31·76	0·855
	25·869	$0{\cdot}8921 \times 10^{-1}$	0·31	1·24	0·3022	13·55	0·796
	29·083	0·2861	0·27	1·10	0·5689	7·954	0·789
	32·480	0·4755	0·25	0·99	0·7741	6·512	0·788
			(b) $\epsilon = 0{\cdot}50$				
2	4·796	0·7563	0·42	0·83	1·086	2·871	1·140
3	5·632	0·6323	0·53	1·06	1·033	3·269	1·095
4	6·799	0·3703	0·59	1·18	0·6567	3·546	0·828
5	8·021	0·2194	0·62	1·25	0·4877	4·447	0·735
6	9·240	0·1278	0·65	1·30	0·3731	5·841	0·687
	12·832	1·1768	0·47	0·94	2·199	3·738	1·132
7	10·444	$0{\cdot}7243 \times 10^{-1}$	0·67	1·34	0·2855	7·882	0·656
	13·823	0·7745	0·51	1·01	1·075	2·776	0·657
8	11·630	$0{\cdot}3993 \times 10^{-1}$	0·69	1·38	0·2162	10·83	0·635
	15·025	0·5326	0·53	1·06	0·8038	3·018	0·568
			(c) $\epsilon = 0{\cdot}75$				
5	6·8903	1·3974	0·73	0·97	1·025	0·978	0·441
6	8·124	1·2176	0·74	0·98	1·057	1·158	0·448
7	9·308	1·0653	0·75	1·00	1·035	1·296	0·438
8	10·467	0·9381	0·76	1·02	0·9971	1·417	0·424

TABLE 2. Accurate values of the frequencies of trapped modes, and response coefficients.

new zeros represent modes which are highly damped compared with those in figure 5*a*. If the search were carried across the negative imaginary axis onto the second sheet of the Riemann surface, other zeros would presumably be found.

The two systems of zeros in figures 5*a* and 5*b* appear somewhat distinct. This is when the contrast in the depths h_1 and h_2 is quite great: $h_1/h_2 = \frac{1}{16}$. Figures 6*a* and 6*b* show similar results when the contrast is less: $h_1/h_2 = \frac{1}{4}$. Then there are already very few trapped modes (cf. tables 1 and 2). The main sequence in figure 6*a* is somewhat further from the real axis, and in figure 6*b* the zeros are

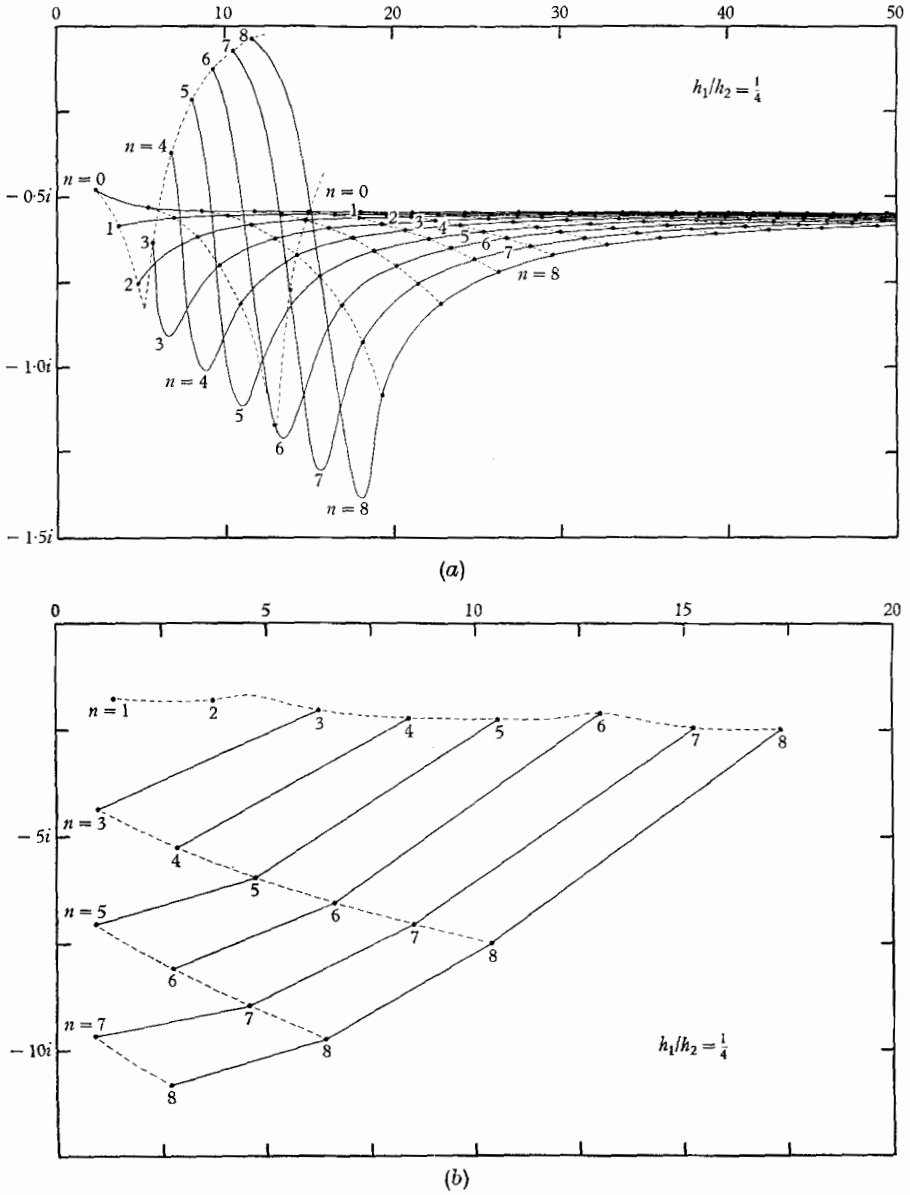

FIGURE 6. The zeros of $G(z)$ when $h_1/h_2 = \frac{1}{4}$: (*a*) the main sequence; (*b*) the remaining zeros.

closer. When the depths are quite comparable, $h_1/h_2 = \frac{9}{16}$, the zeros are as shown in figures 7*a* and 7*b*. The curve marked α in figure 7*a* is the same curve, though on a different vertical scale, as the upper curve in figure 7*b*, so that the two systems of solutions have now been brought together.

The 'second' system of zeros, namely those shown in figures 5*b*, 6*b* and 7*b*, correspond to modes with a high rate of damping. For this reason they are less important in the context of free oscillations, But their existence must be borne in mind in the solution to the problem of forced motions, to be described in the following section.

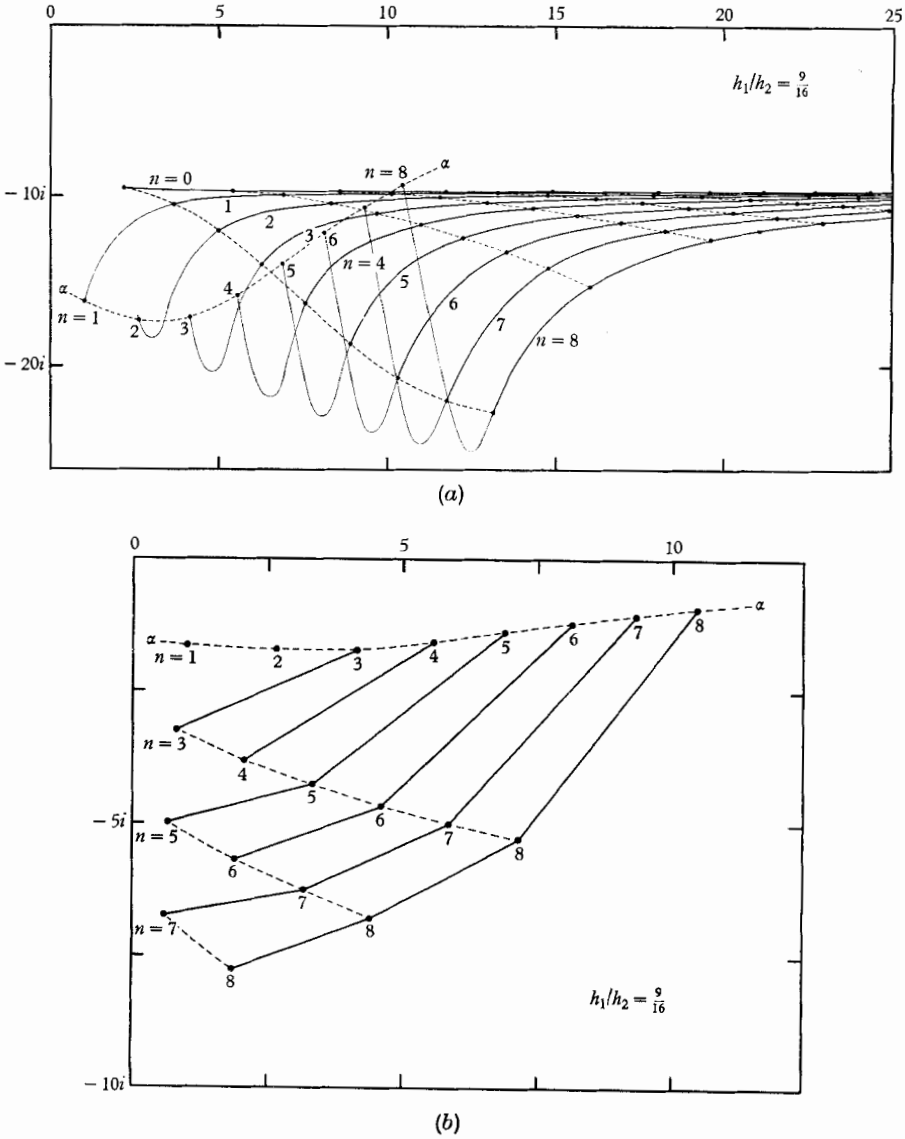

FIGURE 7. The zeros of $G(z)$ when $h_1/h_2 = \frac{9}{16}$; (*a*) the main sequence; (*b*) the remaining zeros.

7. The excitation of trapped modes on a circular sill

It is interesting to enquire how modes of oscillation such as those described in the previous section might be excited by various mechanisms. Among the simplest of such exciting mechanisms is an incident wave propagated from infinity through deep water. In the presence of the sill we shall expect to find part of the incident wave converted to energy over the sill, and part scattered to infinity in the horizontal plane.

Consider for a moment the situation that would be expected according to ray-theory (figure 8). A plane wave approaches in deep water from the left. The ray-paths are parallel until they meet the edge of the sill, where they are refracted both on crossing into the sill and on leaving it. There is a partial focusing of the

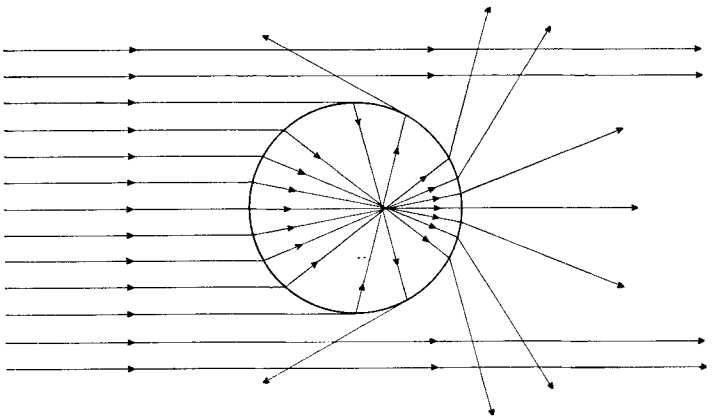

FIGURE 8. The ray-paths for a plane wave incident on a circular sill, when $h_1/h_2 = \frac{1}{16}$.

wave energy. On the other hand the refracted rays over the sill all make an angle with the normal which is less than the critical angle, defined in § 3. Hence they pass closer to the centre of the sill than any of the rays corresponding to the trapped modes. In other words the ray-paths of the incident waves and of the trapped waves cannot coincide over the sill itself.

One might therefore suppose that it would be difficult for an incident wave to excite any of the trapped modes of oscillation. On the other hand the rate of decay of the trapped modes is so small, that even a small input of energy may be sufficient to generate appreciable amplitudes. It is clear that in order to calculate the amplitude of the response we need a more exact analysis than ray-theory can provide.

Let us then consider the response of the system described in § 6 caused by a disturbance which has the form of a plane wave at infinity. Thus suppose that at large distances from the origin $\zeta \sim \zeta_\infty$ where

$$\zeta_\infty = \exp\left[i(k_2 x - \sigma t)\right] \tag{7.1}$$

and σ is real. This by itself satisfies the required differential equation (2.10) in the deeper water $h = h_2$ and so represents a free wave. However, it does not satisfy

the boundary condition (2.6) at $r = a$. Let us expand ζ_∞ in a harmonic series in θ. By a well-known identity, (7.1) can be written

$$\zeta_\infty = \sum_{n=-\infty}^{\infty} i^n J_n(k_2 r) \exp[i(n\theta - \sigma t)]. \tag{7.2}$$

So in place of the free mode (6.1) we now assume

$$\zeta = \sum_{n=-\infty}^{\infty} \exp[i(n\theta - \sigma t)] \times \begin{cases} A_n J_n(k_1 r) & (r < a), \\ B_n H_n(k_2 r) + i^n J_n(k_2 r) & (r > a). \end{cases} \tag{7.3}$$

The terms in A_n represent motions excited over the circular sill, and the terms in B_n represent energy scattered to infinity. On applying the boundary conditions at $r = a$, and equating coefficients of $\exp[i(n\theta - \sigma t)]$ we find

$$\left.\begin{aligned} A_n J_n(k_1 a) &= B_n H_n(k_2 a) + i^n J_n(k_2 a), \\ A_n k_1 h_1 J_n'(k_1 a) &= B_n k_2 h_2 H_n'(k_2 a) + k_2 h_2 i^n J_n'(k_2 a), \end{aligned}\right\} \tag{7.4}$$

and so instead of the homogeneous equations (6.15) we have to solve the non-homogeneous system

$$\begin{pmatrix} J_n(z) & H_n(\epsilon z) \\ \epsilon J_n'(z) & H_n'(\epsilon z) \end{pmatrix} \begin{pmatrix} A_n \\ B_n \end{pmatrix} = i^n \begin{pmatrix} J_n(\epsilon z) \\ J_n'(\epsilon z) \end{pmatrix}. \tag{7.5}$$

Since the frequency σ is real by hypothesis, so also is z, and the matrix of the system cannot vanish. The system (7.5) therefore possesses a unique solution. Making use of the identity

$$J_n(\epsilon z) H_n'(\epsilon z) - J_n'(\epsilon z) H_n(\epsilon z) = \frac{2i}{\pi \epsilon z} \tag{7·6}$$

we find

$$A_n = \frac{2i^{n+1}}{\pi \epsilon G(z)} \tag{7.7}$$

and

$$B_n = i^n \frac{J_n(z) J_n'(\epsilon z) - \epsilon J_n'(z) J_n(\epsilon z)}{F(z)}, \tag{7.8}$$

where $F(z)$ and $G(z)$ are given by (6.16) and (6.17). These values of A_n and B_n, when substituted into (7.3), give the formal solution of the problem.

The modulus of A_n, which represents the amplitude of the waves over the sill in response to an incident wave of unit amplitude, is shown as a function of the non-dimensional frequency $z = a\sigma/(gh_1)^{\frac{1}{2}}$ in figure 9, for the typical case $h_1/h_2 = \frac{1}{16}$. (To avoid confusion, only the even harmonics $n = 0, 2, 4, 6$ are shown.) As can be seen, the response is markedly peaked at values of z close to the zeros of $G(z)$ determined in the previous section, especially those zeros which lie close to the real axis and correspond to trapped modes.

When z lies close to one such value z_0 say, we have approximately

$$G(z) \doteq (z - z_0) G'(z_0) \tag{7.9}$$

and so if $-\eta$ denotes the imaginary part of z_0 ($z_0 = \xi_0 - i\eta$) we have

$$|A_n| \doteq \frac{2}{\epsilon\pi} \frac{1}{[(\xi - \xi_0)^2 + \eta^2]^{\frac{1}{2}} |G'(z_0)|}. \tag{7.10}$$

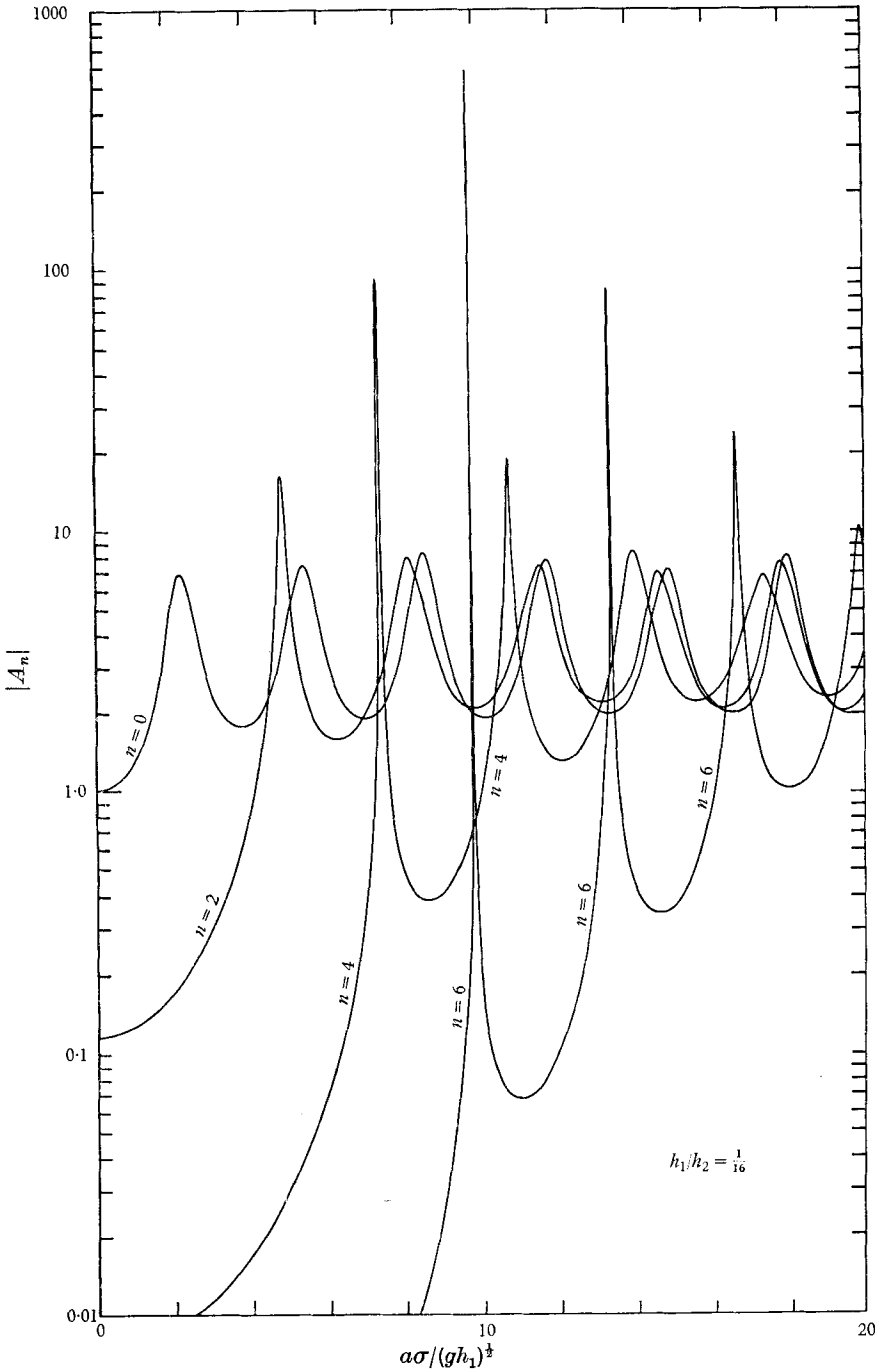

FIGURE 9. Graphs of $|A_n|$, for $h_1/h_2 = \frac{1}{16}$ and $n = 0$, 2, 4 and 6, giving the amplitude of the response as a function of the frequency of the incident wave.

The peak value of the response is thus achieved when $\xi \doteqdot \xi_0$, and

$$\max |A_n| \doteqdot \frac{2}{\epsilon\pi\eta\,|G'(z_0)|}. \tag{7.11}$$

The width of the response curve, that is to say the difference in ξ between points at half the peak height, is $2\sqrt{3}\,\eta$.

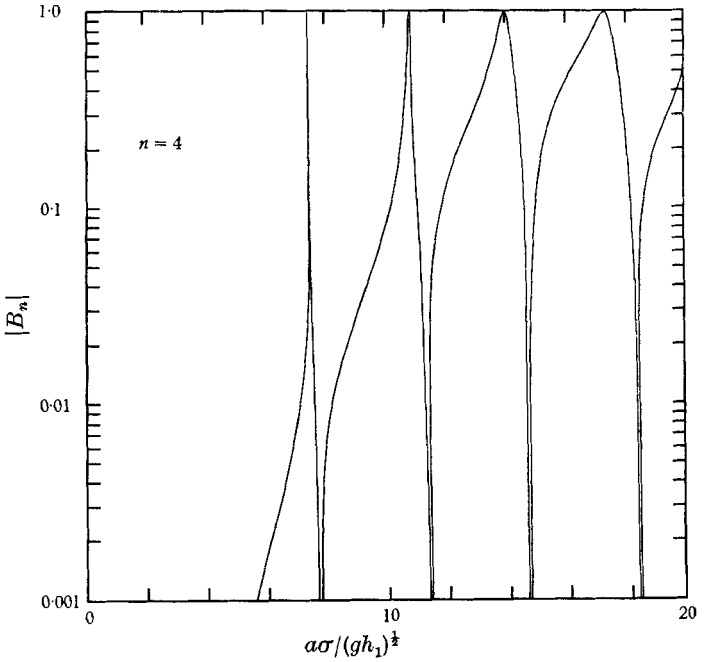

FIGURE 10. Graphs of $|B_n|$ for $h_1/h_2 = \frac{1}{16}$ and $n = 0$, 2, 4 and 6, giving the amplitude of the scattered waves as a function of the frequency of the incident wave.

In terms of the constants

$$D_{nk} = \frac{2i^n}{\pi\,G'(z_k)}, \quad D = |D_{nk}|, \tag{7.12}$$

which occur in § 8, we have

$$\max |A_n| = \frac{D}{\epsilon\eta}. \tag{7.13}$$

Both D and $D/(\pi\eta)$ are given in table 2. From these it can be seen how large are the amplitudes that can be built up inside the sill by the trapping effect; also how narrow are the response curves. It will be recalled that the ordinary transmission coefficient for a long wave approaching a straight step normally (that is to say the ratio of the transmitted wave amplitude to the incident wave amplitude) is $2/(1+\epsilon)$ (see Lamb 1932; Bartholomeusz 1958). In the present instance ($\epsilon = \frac{1}{4}$) this ratio equals 1·6.

The amplitude of each wave in the series (7.3) is also proportional to $J_n(k_1 r)$, that is to say to $J_n(r/a\,.\,z)$ where $z = \xi - i\eta$ is the quantity given in table 2. Now

the maximum value of $J_n(\xi)$ occurs in the neighbourhood of the turning-point $\xi = n$ and is given approximately by

$$\max J_n(\xi) = 0{\cdot}675n^{-\frac{1}{3}} \tag{7.14}$$

(see the appendix). This weak dependence on n does not affect the order of magnitude of the results derived from table 2. Outside the neighbourhood of the critical region $J_n(\xi)$ diminishes like $n^{-\frac{1}{2}}$.

Consider now the scattering coefficient $|B_n|$. The behaviour of $|B_n|$ when $h_1/h_2 = \frac{1}{16}$ and $n = 4$ is shown in figure 10. In contrast to $|A_n|$, it is possible for $|B_n|$ to vanish identically at certain frequencies. The amplitude of the scattered wave is then zero. An analogous effect occurs in the scattering of electrons by rare gas atoms, where it is known as the Ramsauer–Townsend effect (see Schiff 1949, § 109).

The phenomena described in the present section are also very similar to the scattering of underwater sound by a gas bubble. When the frequency of the incident sound wave lies close to the fundamental resonant frequency of the bubble, the amplitude of the induced oscillation may be greatly magnified. However, in contrast to the previous examples, viscosity also plays an important part, resulting in large coefficients of absorption (Albers 1960). The effect of viscous damping in our present problem will be considered in § 11.

8. The response of a circular sill to a travelling pulse

Whereas the problem treated in § 7 was analogous to the excitation of an acoustical resonator or a bell by a sound of constant pitch, it may be interesting also to investigate the response of the circular sill to a travelling pulse. This corresponds to striking the bell with a shock wave.

A straight line-pulse travelling in the x-direction ($\theta = 0$) in water of depth h_2 may be represented by

$$\zeta_\infty = (1/\sigma_2)\,\delta(x/c_2 - t), \tag{8.1}$$

where

$$c_2 = (gh_2)^{\frac{1}{2}}, \qquad \sigma_2 = c_2/a \tag{8.2}$$

and $\delta(t)$ denotes the Dirac delta-function. The latter may be represented by the improper integral

$$\delta(t) = \frac{1}{2\pi}\int_C e^{-i\sigma t}\,d\sigma, \tag{8.3}$$

where C denotes the contour running from $-\infty$ to ∞ just above the real axis, as in figure 11. The response of the system to such a pulse can be written down immediately from the solution of the previous section. We shall consider only the disturbance over the sill ($r < a$). This is given by

$$\zeta = \sum_{n=-\infty}^{\infty} P_n(r,t)\,e^{in\theta}, \tag{8.4}$$

where

$$P_n(r,t) = \frac{1}{2\pi\sigma_2}\int_C A_n J_n(k_1 r)\exp(-i\sigma t)\,d\sigma \tag{8.5}$$

and A_n is given by (7.7). Thus, in the notation of § 7, we have

$$P_n(r,t) = \frac{i^{n+1}}{\pi^2}\int_C \frac{J_n(zr/a)}{G(z)}\exp(-iz\bar{t})\,dz, \tag{8.6}$$

where

$$\bar{t} = \sigma t/z = t(gh_1)^{\frac{1}{2}}/a \tag{8.7}$$

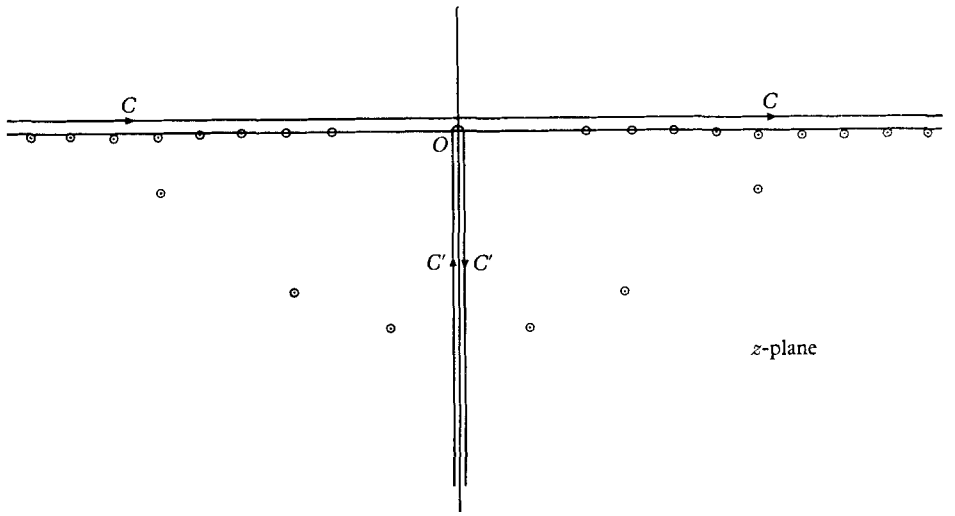

FIGURE 11. A sketch of the contours C and C' and of the zeros of $G(z)$ when $h_1/h_2 = \frac{1}{16}$ and $n = 6$.

and z denotes $\sigma a/(gh_1)^{\frac{1}{2}}$ as before.

The integrand is regular everywhere except for poles at the zeros of $G(z)$, and for a logarithmic irregularity at the origin. All the poles lie below the real axis, and the plane is usually cut from 0 to $-\infty$. When $\bar{t} < -1$ the integrand can be deformed into an infinite semicircle in the upper half-plane and vanishes identically. When $\bar{t} > 1$ the integrand can be deformed into an infinite semicircle in the lower half-plane, minus $2\pi i$ times the residues at the poles of the integrand, plus an integral along the path C' running up the negative real axis on the second sheet of the Riemann surface and down the imaginary axis on the first sheet, as in figure 11. Thus we have

$$P_n(r,t) = \sum_k D_{nk}\,J_n(r/az_k)\exp(-iz_k\bar{t}) + R_n, \tag{8.8}$$

where

$$D_{nk} = \frac{2i^n}{\pi G'(z_k)} \tag{8.9}$$

and

$$R_n = \frac{i^{n+1}}{\pi^2}\int_{C'} \frac{J_n(r/a.z)}{G(z)}\exp(-i\bar{t}z)\,dz. \tag{8.10}$$

The summation with respect to k extends over all the zeros z_k of $G(z)$. Thus equation (8.8) expresses the response to the impulse as the sum of a number of free waves of amplitude

$$D = |D_{nk}| \tag{8.11}$$

each decaying exponentially in time (since $\mathscr{I}(z_k) < 0$) plus a remainder term R_n which represents a transient 'tail'.

The amplitudes D of the decaying modes are tabulated in table 2.† To evaluate R_n asymptotically for large values of $\bar{t}$ we note that near $z = 0$ we have

$$\left.\begin{aligned} G(z) &= P \pm Q, \\ \text{where} \qquad P &\sim \frac{i(1+\epsilon^2)}{\pi\epsilon^{n+1}}, \quad Q \sim \frac{\epsilon^{n-1}(1-\epsilon^2)z^{2n}}{2^{2n-1}n!\,(n-1)!} \end{aligned}\right\} \tag{8.12}$$

and the positive or negative sign is to be taken according as z lies to the right or left of the imaginary axis. Thus

$$\frac{1}{G(z)} \sim \frac{1}{P} \mp \frac{Q}{P^2}.$$

Since

$$J_n(r/a.z) \sim \frac{(r/a.z)^n}{2^n n!} \tag{8.13}$$

it follows by Watson's lemma that as $\bar{t} \to \infty$,

$$\begin{aligned} R_n &\sim \frac{2i^{n+1}}{\pi^2}\int_o^{-i\infty} \frac{(r/a)^n z^n}{2^n n!}\frac{Q}{P^2} e^{-i\bar{t}z}\,dz \\ &= \frac{4(3n)!}{(n!)^2(n-1)!}\left(\frac{-\epsilon}{2}\right)^{3n}\frac{\epsilon(1-\epsilon^2)}{(1+\epsilon^2)^2}\left(\frac{r}{a}\right)^n \frac{1}{\bar{t}^{3n+1}}. \end{aligned} \tag{8.14}$$

Thus R_n dies away asymptotically like $t^{-(3n+1)}$. For moderately large values of $\bar{t}$ this transient tail will be much less than the amplitudes of the slowly decaying trapped modes.

9. Wave trapping round islands of more general shape

In the following section we shall consider whether the phenomenon of wave trapping, which has been demonstrated for the circular sill, is displayed also when the topography of the sea floor is of a more general kind.

(i) *Circular island with sill*

Suppose that a meridional section of the island is as shown in figure 12, that is to say a central island of radius b surrounded by a circular sill of radius a and depth h_1, beyond which is deep water of depth $h_2 > h_1$. We have seen already that in the absence of the central island it is possible to have waves trapped on the shelf and that in such modes there is very little energy inside the inner critical circle, of radius n/k_1 where $k_1 = \sigma/(gh_1)^{\frac{1}{2}}$. Hence if $b < n/k_1$, that is to say if the radius of the island is less than the inner critical radius, its presence will have little effect on that particular mode. In other words we may infer the existence of trapped modes of oscillation in the presence of the central island as well as in its absence. For any radius b, provided it is less than a, the ray theory indicates that such modes will exist, though when b approaches a (that is to say if the shelf is relatively narrow) then for a trapped mode to exist n would have to be large.

† When $n > 0$ the contribution from terms $P_{-n}(r, t)$ duplicates that from $P_n(r, t)$ so the amplitudes must be multiplied by 2.

Although some of the free modes might not be affected by the presence of the island, the latter will certainly affect the detailed generation of these modes by a travelling pulse as described in § 8, or by another such mechanism, for the island would necessarily intersect the ray paths of the incident waves.

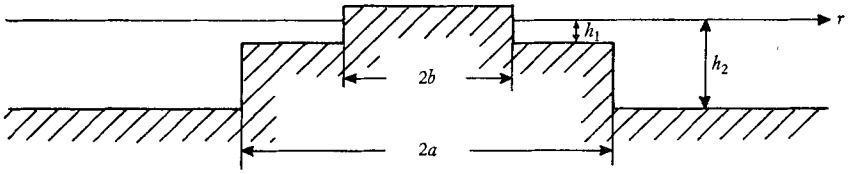

FIGURE 12. Cross-section of an island with a surrounding sill.

It should also be pointed out that the presence of the island may make possible the existence of other types of trapped modes, namely those whose rays are reflected both internally at the edge of the sill and at the shoreline.

(ii) *Circular symmetry; the general case*

Next let us suppose that the depth h is a more general function of the radius r (but still independent of θ). Under what conditions may we expect trapped oscillations? Consider first a ray trajectory at some point where the path is locally transverse, that is to say the wave crests are parallel to the local radius vector. Then for the ray to be refracted inwards it is clearly necessary that the curvature of the trajectory be greater than the curvature of a circle with radius r. This leads to the condition

$$\frac{1}{c}\frac{\partial c}{\partial r} > \frac{1}{r}, \tag{9.1}$$

where c is the local speed of propagation. Hence

$$\frac{\partial}{\partial r}\left(\frac{c}{r}\right) > 0 \tag{9.2}$$

or since in this case $c = (gh)^{\frac{1}{2}}$ we have

$$\frac{\partial}{\partial r}\left(\frac{h}{r^2}\right) > 0. \tag{9.3}$$

In other words the depth must increase more rapidly than the square of the radius. This conclusion is also in agreement with the analysis of § 5. For if h/r^2 increases without limit then coefficient of R in equation (5.4) or (5.5) must ultimately become negative.

A zone in which equation (9.3) is satisfied is then capable of refracting waves back towards the centre. Such a zone may be called a 'hedge'. Clearly any discontinuity in depth, with the greater depth on the outside, is a limiting form of 'hedge'. (Every 'edge' is a 'hedge'.) As we have seen, hedges are not entirely inpenetrable, since generally there is a fringe of radiation on the outside. Moreover, hedges are effective only when the angle of incidence exceeds a certain critical

angle. Nevertheless, in the case of circular symmetry a ray once refracted back towards the centre by a hedge must ultimately approach the hedge again at the same angle. Hence the energy will be contained with only a small leak of energy to the outside.

The concept of a hedge is evidently equivalent to that of a potential barrier in quantum mechanics. In this connexion Eckart (1951) has drawn attention to the exact analogy between the ray-paths described by waves propagated with velocity $(gh)^{\frac{1}{2}}$ and the paths described by a smooth particle sliding freely on the reciprocal surface $\zeta = -1/h$, provided that the object starts with the kinetic energy that would be acquired in falling from the level $\zeta = 0$.

(iii) *Effects of asymmetry*

In more general forms of bottom topography a sufficient condition for trapping of wave energy appears to be the existence of at least one continuous ray-path surrounding the island. However, the curvature of the ray-path must not be so great that appreciable energy is lost at the sharp corners by diffraction.

In the case of *slight* departure from circular symmetry an interesting phenomenon appears in the form of a splitting of the frequencies into slightly different pairs. A simple analogue is the slightly asymmetrical bell, discussed by Rayleigh (1945, chapter 10). Consider, for example, a standing-wave mode (in a bell with perfect circular symmetry) which has an azimuthal wave-number $n = 2$. The form of the bell when oscillating in such a mode will be an ellipse of small eccentricity, with nodal planes at, say, $\theta = 0$, $\frac{1}{2}\pi$, π and $\frac{3}{2}\pi$. There will exist a second and similar standing mode with nodal planes relatively displaced by $\frac{1}{4}\pi$, that is to say at $\theta = \frac{1}{4}\pi$, $\frac{3}{4}\pi$, $\frac{5}{4}\pi$ and $\frac{7}{4}\pi$. The frequencies of the two modes will be equal. Suppose now that a small mass is added to the bell at the point $\theta = 0$. This will not affect the radial motion† of the bell in the first mode nor the elastic restoring force. But, lying at an antinode of the second mode, it will increase the inertia in the second mode. Hence the frequencies of the two modes will be split. In a similar way, any slight asymmetry in the circular shape of an island or sea mount will result in slight differences in the inertia of pairs of modes whose nodal lines are displaced relative to one another. Hence we expect the existence of pairs of modes of the same azimuthal wave-number n and radial wave-number m, but of slightly different frequencies.

The modes just described are stationary, that is to say they have fixed nodal lines (where the radial displacement vanishes). Denote one such pair by ζ_1 and ζ_2 respectively. Suppose that these are of equal energy. Consider now the motions consisting of the sum of the two modes, in quadrature. That is to say let

$$\zeta_+ = \zeta_1 + i\zeta_2, \quad \zeta_- = \zeta_1 - i\zeta_2. \tag{9.4}$$

Since ζ_1 and ζ_2 represent standing waves it follows that ζ_+ represents a progressive wave travelling round the centre in the clockwise direction, say; and ζ_- represents a wave travelling in the anticlockwise sense. But because the frequencies are slightly different the phase difference between ζ_+ and ζ_- will slowly change.

† However, the transverse inertia will be affected.

Hence ζ_+ will eventually be converted to ζ_- and vice versa. In other words there will be an exchange of energy between the progressive modes; the effect of slightly asymmetry is to introduce a coupling between them.

We may show that under certain circumstances the frequency splitting due to a slight asymmetry will be of second-order in the deformation of the island. Imagine a sill of uniform depth, as in § 6, whose edge is given not by $r = a$ but by

$$r = a(1 + \eta \cos p\theta), \tag{9.5}$$

where η is a small quantity and p is an integer $\geqslant 2$. Consider a mode which in the case of circular symmetry has an azimuthal wave-number n. Then, in the case of symmetry, the ray-paths will meet the edge of the sill at points given by

$$r\,e^{i\theta} = a \exp[i(2\pi k/n + \beta)], \tag{9.6}$$

where β is a constant and k is an integer running from 1 to n. In the asymmetrical case, the inter-reactions of the ray-path with the edge of the sill will be given by

$$r\,e^{i\theta} = a(1 + \eta \cos p\theta_k) \exp(i\theta_k), \tag{9.7}$$

where the θ_k are angles which differ, in general, from $(2\pi k/n + \beta)$ by amounts of order η. It is easy to see that when $n > 2$ the difference in the total path length caused by replacing θ_k by $(2\pi k/n + \beta)$ is of order η^2. Then, by writing down the expression for the total path-length and using the fact that

$$\sum_{k=1}^{n} \exp(2\pi pki/n) = n \quad \text{or} \quad 0 \tag{9.8}$$

according as p is or is not a multiple of n, it can be shown that the total path-length differs from the path-length in the case $\eta = 0$ by an amount of order η^2, except when p is a multiple of n.

We infer that the frequency splitting due to asymmetry is of the second-order in the deformation η^2, except possibly when the azimuthal wave-number n of the mode is a submultiple of one of the harmonics p involved in the asymmetry of the island.

This is easily verified by geometrical methods in the case when the island is of elliptical shape ($p = 2$) and the mode considered has a wave-number n equal to 4.

A more precise calculation of the frequency splitting due to asymmetry will be given in another paper.

10. Effects of the earth's rotation

In this section we shall investigate briefly the effect on these long waves of coriolis forces due to the rotation of the earth.

One effect of the rotation is suggested by an investigation due to Reid (1958) who calculated the effect of coriolis forces on edge waves over a bottom of uniform gradient. He found that in the northern hemisphere gravity waves travelling with the shoreline to their left have their speed of propagation increased by the earth's rotation, and those with the shoreline on their right have their speed diminished. Hence, we may expect that waves travelling round a circular island in the same direction as the earth's rotation will have their speed increased

(relative to the earth), and those travelling in the opposite direction will have their speed diminished. Thus we expect the earth's rotation to split the frequencies of pairs of progressive modes (just as the assymmetry splits the frequencies of pairs of standing modes).

To pursue the present problem analytically, we note that the general equations corresponding to (2.1) and (2.2) but with the coriolis forces included, are

$$\left.\begin{aligned}\frac{\partial u}{\partial t}-fv &= -\frac{\partial}{\partial x}(g\zeta),\\ \frac{\partial v}{\partial t}+fu &= -\frac{\partial}{\partial y}(g\zeta),\end{aligned}\right\} \tag{10.1}$$

where f denotes the coriolis parameter. The continuity equation (2.2) is the same as before. Assuming that u, v and ζ are proportional to $e^{-i\sigma t}$ we have from (10.1)

$$\left.\begin{aligned}-i\sigma u-fv+\frac{\partial}{\partial x}(g\zeta) &= 0,\\ fu-i\sigma v+\frac{\partial}{\partial y}(g\zeta) &= 0,\end{aligned}\right\} \tag{10.2}$$

whence

$$\left.\begin{aligned}u &= \frac{-i\sigma g}{\sigma^2-f^2}\left(\frac{\partial}{\partial x}-\frac{f}{i\sigma}\frac{\partial}{\partial y}\right)\zeta,\\ v &= \frac{-i\sigma g}{\sigma^2-f^2}\left(\frac{f}{i\sigma}\frac{\partial}{\partial x}+\frac{\partial}{\partial y}\right)\zeta,\end{aligned}\right\} \tag{10.3}$$

and so on substituting in (2.2)

$$\left(\nabla^2+\frac{\sigma^2-f^2}{gh}\right)\zeta+\frac{1}{h}\nabla h.\nabla\zeta-\frac{f}{i\sigma}\frac{1}{h}(\hat{\mathbf{w}}.\nabla h\wedge\nabla\zeta), \tag{10.4}$$

where $\mathbf{w}$ denotes a unit vector in the z-direction. At a discontinuity in the depth the boundary conditions are that

$$\zeta \text{ is continuous} \tag{10.5}$$

and that $h\mathbf{u}.\mathbf{n}$ is continuous. From (10.3) this implies

$$h\left(\frac{\partial\zeta}{\partial n}-\frac{f}{i\sigma}\frac{\partial\zeta}{\partial s}\right) \text{ is continuous,} \tag{10.6}$$

where n, s are measured normally and tangentially to the discontinuity in the same right-handed sense as x, y. We shall see that the additional term in (10.6) is of particular significance.

In the special case of water which is of locally uniform depth, (10.4) reduces to

$$\left(\nabla^2+\frac{\sigma^2-f^2}{gh}\right)\zeta = 0. \tag{10.7}$$

Supposing that the period of the oscillations is small compared to a pendulum day, we shall have $\sigma \gg f$. In the following we shall agree to take into account quantities of order f/σ but to neglect those of order $(f/\sigma)^2$. It is clear then that

under these conditions (10·7) reduces simply to the equation (2.10) for long waves in the absence of rotation. However, the boundary condition (10.6) introduces a first-order difference.

Consider first a straight step or discontinuity in depth as in § 3, and let us assume a solution in the form (3.4). The boundary conditions (10.5) and (10.6) now give $A = C$ and

$$h_1[l_1 B - m(f/\sigma) A] = h_2[-l_2' - m(f/\sigma)] C. \tag{10.8}$$

Therefore altogether we find

$$\zeta = \exp[i(my - \sigma t)] \times \begin{cases} l_1 h_1 \cos l_1 x - [l_2' h_2 + m(f/\sigma)(h_2 - h_1)] \sin l_1 x & (x < 0), \\ l_1 h_1 e^{-l_2' x} & (x > 0). \end{cases} \tag{10.9}$$

The effect of the additional term on the right of (10.9) is to increase the phase δ of the waves just inside the edge of the sill by an amount

$$\delta' = \frac{m(f/\sigma)(h_2 - h_1) l_1 h_1}{(l_1 h_1)^2 + (l_2' h_2)^2}. \tag{10.10}$$

This extra phase must then be accommodated over the sill. Similarly on inserting the boundary condition $u = 0$ at $x = -a$ we find that an additional phase

$$\delta'' = \frac{m(f/\sigma)}{l_1} \tag{10.11}$$

must be accommodated at the other side of the sill. Hence, if the frequency of the waves were to remain unchanged the width of the sill would have to be increased by an amount $(\delta' + \delta'')/l_1$. The actual change in frequency will be the same as if the width of the sill were *de*creased by this amount. Now the effect of decreasing the width of the sill (in the absence of coriolis forces) will be to increase the frequency, in general. Hence if $(\delta' + \delta'')$ is positive the frequency must be increased.

Now if m, f and σ are all positive, that is to say if the waves travel in the positive y-direction in the northern hemisphere, then from (10.10) and (10.11) we see that δ' and δ'' are both positive. Hence, in the northern hemisphere, those waves which progress along the shore with the shoreline to their left have their frequency increased, and those which travel in the reverse sense have their frequency diminished, in agreement with the result of Reid (1958) for a uniformly sloping bottom.

Consider now the effect of rotation on the sill waves discussed in § 6. We may estimate the wave frequency by an equation analogous to (6.10). In fact we have only to add to the right-hand side of (6.10) the term

$$\frac{(h_2 - h_1) m(f/\sigma)}{l_1 h_1}, \tag{10.12}$$

where

$$m = n/a = l_1 \cot u \tag{10.13}$$

by (6.8). Hence we have as an approximate equation

$$\tan [n(\tan u - u) - \tfrac{1}{4}\pi] = \sqrt{[(h_2/h_1)\{(h_2/h_1 - 1)\cot^2 u - 1\}]} + (f/\sigma)(h_2/h_1 - 1)\cot u. \tag{10.14}$$

From figure 3 it is clear that when $0 < f/\sigma \ll 1$ the effect of the last term is to increase the value of u by an amount nearly proportional to f/σ; and therefore to increase σ, by equation (6.11). Hence the speed of waves travelling in the anticlockwise direction is increased, and the speed of waves travelling in the clockwise direction is decreased, as was expected.

To find the small difference $\Delta\sigma$ in the frequency due to the Earth's rotation we note that since σ, by (6.11), is proportional to $\sec u$ we have

$$\frac{\Delta\sigma}{\sigma} = \tan u\, \Delta u. \tag{10.15}$$

The corresponding increment Δu is found from the relation

$$\frac{dF_1}{du}\Delta u = \frac{dF_2}{du}\Delta u + (f/\sigma)(h_2/h_1 - 1)\cot u, \tag{10.16}$$

where F_1 and F_2 denote the functions on the left and right of (6.10) and u is one of the roots of (6.10). From the last two equations we deduce that

$$\Delta\sigma = \frac{(h_2/h_1 - 1)f}{dF_1/du - dF_2/du}. \tag{10.17}$$

On carrying out the differentiation we find, after some reduction,

$$\Delta\sigma = \frac{f}{n(\gamma - s + 1) + \dfrac{s}{s-1}\left(\dfrac{\gamma}{\gamma - s}\right)^{\frac{1}{2}}}, \tag{10.18}$$

where

$$\gamma = h_2/h_1, \quad s = \sec^2 u = (\xi/n)^2. \tag{10.19}$$

It will be noted that as $n \to \infty$ leaving γ and s constant, the 'beat frequency' $\Delta\sigma$ is asymptotically proportional to f/n.

The values of $\Delta\sigma/f$ corresponding to the frequencies already calculated in table 1 are shown in table 3.

	$n =$							
h_1/h_2	1	2	3	4	5	6	7	8
	0·1263	0·0426	0·0252	0·0179	0·0139	0·0114	0·0096	0·0079
	—	0·1200	0·0432	0·0248	0·0175	0·0136	0·0111	0·0094
$\frac{1}{16}$	—	—	0·0832	0·0462	0·0254	0·0176	0·0135	0·0110
	—	—	—	0·0000	0·0505	0·0266	0·0180	0·0136
	—	—	—	—	—	0·0549	0·0282	0·0186
	—	—	—	—	—	—	0·0580	0·0302
$\frac{1}{4}$	—	0·1189	0·1176	0·0890	0·0685	0·0549	0·0457	0·0389
	—	—	—	—	—	0·0400	0·0700	0·0630
$\frac{9}{16}$	—	—	—	—	0·0282	0·0540	0·0789	0·0797

TABLE 3. Changes in the frequencies of trapped modes of oscillation due to the rotation of the earth: values of $\Delta\sigma/f$

It is interesting to compare these results with those for a bell rotating about its axis of symmetry. Bryan (1890) calculated the effect of rotation on the normal modes of a cylindrical bell. He found that if Ω denotes the angular velocity of the

bell about its axis, then the nodal lines of the oscillation follow the direction of rotation but with a smaller angular velocity given by

$$\frac{n^2-1}{n^2+1}\Omega, \tag{10.20}$$

where n is the azimuthal wave-number. Thus, relative to an observer in the rotating frame (as on the rotating earth) the nodal lines tend to drift in the opposite direction to the rotation, with angular velocity

$$\frac{-2\Omega}{n^2+1}. \tag{10.21}$$

If these standing oscillations are considered as the sum of two progressive oscillations, one travelling in the same sense as Ω and the other in the opposite sense, then it follows that the frequency of the mode progressing in the same sense as the basic rotation is slowed down (in the rotating frame of reference) by an amount equal to

$$\frac{2n\Omega}{n^2+1}. \tag{10.22}$$

Thus in the case of a rigid bell, the effect of the coriolis forces on the phase velocity is in the reverse sense, compared with the effect on edge waves. The magnitude of the frequency shift for large n is however similar. For since f is of order 2Ω, we see from (10.22) that the change in frequency due to the rotation is again of order f/n.

Combining the results of the present section with those of § 9 we can now see qualitatively what is the effect on free waves of coriolis forces and of slight asymmetry present simultaneously. The coriolis forces induce a slight difference in frequency between the modes progressing round the island in the clockwise and in the anticlockwise sense, those in the anticlockwise sense travelling faster, in the northern hemisphere. The asymmetry of the island induces an exchange of energy between these two progressive modes.

Consider then a record of the surface elevation as seen by a fixed observer. If there were no asymmetry, then in a given small frequency band he would see in general the sum of two waves of slightly differing frequencies:

$$\zeta = A_1 \cos[(\sigma+\Delta\sigma)t+\epsilon_1]+A_2\cos[(\sigma-\Delta\sigma)t+\epsilon_2], \tag{10.23}$$

where A_1, A_2 and ϵ_1, ϵ_2 represent the instantaneous amplitudes and phases of the waves travelling in the anticlockwise and clockwise senses. When A_1 and A_2 were equal the record of ζ would exhibit slow beats of frequency $\Delta\sigma$.

If now the island is unsymmetrical there will be a slow exchange of energy between the two modes, so that A_1, A_2 and ϵ_1, ϵ_2 will themselves vary with a slow frequency $\Delta'\sigma$, say. Thus at one epoch the wave record may exhibit only waves of frequency $(\sigma+\Delta\sigma)$ and at another epoch it may exhibit only waves of frequency $(\sigma-\Delta\sigma)$. If, however, $\Delta'\sigma \ll \Delta\sigma$ that is to say if the effect of asymmetry is only slight compared with the effect of rotation, then there will still be an epoch when $A_1 \doteqdot A_2$ and beats are observed. If $\Delta'\sigma$ is not small compared with $\Delta\sigma$ the combined motion is more complicated.

In the above discussion we have of course neglected the damping of the waves, which may be important in practice.

11. Effects of viscous damping

Since the amplitude of the trapped modes excited by an incident wave is critically dependent on the loss of energy to infinity, which may be very small, it is important to consider the effect on the waves of other energy losses, in particular the loss due to viscous dissipation.

Suppose first that the flow is laminar. In shallow water, the principal loss of energy will take place in the boundary layer near the bottom. If u_0 denotes the horizontal velocity just outside the boundary layer ($u_0 \propto e^{-i\sigma t}$) then it is easy to show (cf. Lamb 1932) that the horizontal velocity within the layer is given by

$$u = u_0(1 - e^{-\alpha z}), \tag{11.1}$$

where

$$\alpha = (-i\sigma/\nu)^{\frac{1}{2}}, \quad \mathscr{R}(\alpha) > 0, \tag{11.2}$$

z is the vertical distance above the bottom and ν denotes the kinematical viscosity. The rate of dissipation of energy per unit horizontal area of the bottom is given by

$$\dot{E} = \int_0^\infty \rho\nu \overline{\left(\frac{\partial u}{\partial z}\right)^2} \, dz \tag{11.3}$$

and on substitution for u and taking mean values with respect to the time t we find

$$\dot{E} = \frac{1}{2\sqrt{2}} \rho \, |u_0^2| \, (\nu\sigma)^{\frac{1}{2}}. \tag{11.4}$$

On the other hand the mean kinetic energy in a vertical column of unit section is given by

$$\tfrac{1}{4}\rho |u_0^2| \, h. \tag{11.5}$$

The total mean energy E per unit area is twice this. Hence we have

$$\frac{\dot{E}}{\sigma E} = \frac{1}{\sqrt{2}} \frac{(\nu/\sigma)^{\frac{1}{2}}}{h}. \tag{11.6}$$

This quantity is proportional to the loss of energy per unit cycle. It is of the same order of magnitude as the ratio of the boundary-layer thickness $(\nu/\sigma)^{\frac{1}{2}}$ to the mean depth h.

The quantity (11.6) is to be compared with the ratio η/ξ in table 2. Only if (11.6) is small compared with η/ξ can the viscous damping be neglected.

Consider for example waves of period 6 minutes in water of depth $h = 100\,\text{m}$ (the assumed depth of water over the sill). Then $\sigma \doteqdot 0{\cdot}017\,\text{sec}^{-1}$, and since $\nu = 0{\cdot}01\,\text{cm}^2/\text{sec}$ it follows that $(\nu/\sigma)^{\frac{1}{2}}/h$ is of order 10^{-4}. Inspection of table 2 then shows that there may indeed be some trapped modes for which the viscous damping, if laminar, is negligible.

If, on the other hand, the motion is turbulent, due to the roughness of the bottom or the magnitude of the wave amplitude or to the presence of other strong currents, then the wave damping may well be increased by one or two orders of magnitude. Hence the existence of trapped modes of appreciable amplitude will in practice depend somewhat on the circumstances.

12. The response to a broad-band spectrum.

In § 7 we calculated the response of the waves over a circular sill to radiation of a particular frequency falling on it from infinity. However, the background radiation in the ocean more probably has a continuous spectrum. Let us then consider the response of the waves on the sill in that case.

Let $E_\infty(\sigma)$ denote the spectral density of the waves in the deeper water, that is to say, let the contribution to the mean square wave-height $\overline{\zeta^2}$ from frequencies in the range $(\sigma, \sigma+d\sigma)$ be equal to $E_\infty(\sigma)\,d\sigma$. If we neglect for a moment the viscous damping and the effects of asymmetry and coriolis forces, then by § 7 the spectral density $E(\sigma)$ of waves over the sill is of the same order as

$$2E_\infty(\sigma)\,|A_n J_n|^2. \tag{12.1}$$

(The factor 2 arises from the presence of two waves, one travelling round the island in each direction.) This is the spectral density that would theoretically be measured by a very sharply-tuned filter. If we replace $|A_n^2|$ by its approximate value (7.13) and integrate over the resonant peak, assuming E_∞ locally constant, we obtain for the total energy in the band:

$$2\pi \frac{\sigma_1 E_\infty}{\eta}\left|\frac{DJ_n}{\epsilon}\right|^2, \tag{12.2}$$

where $\sigma_1 = (gh_1)^{\frac{1}{2}}/a$. Supposing this energy were distributed over the whole frequency range $(0, 2\sigma)$, the mean spectral density would still be

$$\pi \frac{E_\infty}{\xi\eta}\left|\frac{DJ_n}{\epsilon}\right|^2. \tag{12.3}$$

The quantities $D/\epsilon(\xi\eta)^{\frac{1}{2}}$ are given in the last column of table 2. Since these are all of order unity it is evident that even with a very broad-band filter the response would still be prominent.

Even if the effective value of η is increased by dissipation, (resulting in a decrease in the 'Q' of the resonant system) the r.m.s. amplitude of the resonant response will be diminished only by a factor $\eta^{-\frac{1}{2}}$. Hence the existence of a fairly large energy dissipation will not necessarily be fatal to the detection of the trapped modes.

13. Discussion and conclusions

We have seen how free modes of oscillation over a circular sill are possible, with only a very slow leakage of energy to infinity. The trapping of the energy is essentially due to the waves being reflected internally at the edge of the sill, when their angle of incidence is greater than the critical angle. A necessary condition for this trapping is that the outer critical circle shall be appreciably larger than the circular sill.

The trapping effect is not limited to circular sills, or to islands of circular shape. A sufficient condition for trapping is that there shall be a closed ray-path completely surrounding the island. The presence of an island in the middle of the

shelf or sill does not affect the oscillations, if its radius is less than the inner critical radius (see table 2).

We have also seen how very large can be the response of the water over a sill to waves incident from outside. Even in the presence of viscous damping, the response of the sill to a continuous noise background may still be quite detectable visually. On the other hand the background of low-frequency radiation in the ocean is not yet well known, so that it is not possible to estimate $E_\infty(\sigma)$.

An additional source of energy for trapped oscillations might be the action of horizontal wind-stresses, which are known to be more effective in shallow water. It is also possible that surf-beats of period 2–5 min may contribute some energy at the higher frequencies.

We have seen that any departure from circular symmetry will produce a coupling between the energy of waves travelling round the island in opposite senses. The rotation of the earth will split the frequencies. The splitting is small; the beat frequency due to rotation is of order $(h_1/h_2)\,(f/n)$ where f is the coriolis parameter.

From table 2 it can be seen that when $h_1/h_2 = \frac{1}{16}$ a fair degree of trapping is achieved only if the azimuthal wave-number n is greater than about 4. Hence it appears that the prominent oscillations at Macquarie Island, previously referred to, which had a regular period of 6 min may represent trapped oscillations of this kind. The circumference C of the island being 80 km and the mean depth h_1 of water over the shelf being about 100 m we expect the period of oscillations prominent at the shore to be given by

$$\frac{C}{n(gh_1)^{\frac{1}{2}}} = \frac{80\,\text{km}}{32n\,\text{m/sec}} = \frac{42}{n}\,\text{minutes}.$$

With n equal to about 7 this gives a period of the same order as that observed.

On the other hand table 3 indicates that in this case the splitting of the frequencies due to the rotation of the earth would be too small to account for the observed beat frequency of 0·33 cycles per hour. Hence the observed beats are more likely to be due to other causes. For example, since the ratio of the length of the island to its breadth is about 6:1, the asymmetry is probably important.

Before any firm conclusions are drawn regarding the nature of the oscillations at Macquarie Island it is desirable to repeat the observations over a longer period of time, and further, to make simultaneous observations at more than one point on the coast in order to observe the relative phase of the oscillations. Such observations are at present being undertaken by members of the University of Adelaide.

Other desirable investigations include the accurate calculation of the frequency splitting due to non-circular symmetry, and possibly the construction of a physical model of the island in which the local bathymetry could be more accurately represented.

It is a pleasure to record my thanks to members of the Department of Mathematics at the University of Adelaide for their hospitality from August to November 1964, and particularly to Professor R. B. Potts, Professor J. R. M.

Radok and Dr M. N. Brearley. A first draft of this paper was prepared at Adelaide. For assistance with the calculations in tables 1 and 2 and for several useful suggestions incorporated in this paper I am indebted to Mr C. J. R. Garrett of Trinity College, Cambridge.

Appendix. The maximum value of $|J_n(\xi)|$

In the neighbourhood of the critical point $\xi = n$ it can be shown† that as $n \to \infty$,

$$J_n(\xi) \sim \left(\frac{2}{n}\right)^{\frac{1}{3}} \mathrm{Ai}\,[2^{\frac{1}{3}}n^{\frac{2}{3}}(1-\xi/n)], \tag{A 1}$$

where Ai denotes the Airy function of the first kind (Miller 1964). The maximum value of $|\mathrm{Ai}\,(x)|$ is achieved when $x = -1{\cdot}019$ and $\mathrm{Ai}\,(x) = 0{\cdot}5357$. So we have asymptotically

$$\max|J_n| \sim 0{\cdot}6749n^{-\frac{1}{3}} \tag{A 2}$$

achieved when

$$\xi \sim n + 0{\cdot}809n^{\frac{1}{3}}. \tag{A 3}$$

The actual and asymptotic values of $\max|J_n|$ are compared in table 4. From the agreement between these values it appears that $\max|J_n|$ decreases very nearly as $n^{-\frac{1}{3}}$, between $n = 1$ and $n = 8$.

n	$\max\|J_n\|$	$0{\cdot}6749n^{-\frac{1}{3}}$	ξ	$(n+0{\cdot}809n^{\frac{1}{3}})$
0	1·0000	∞	0·000	0·000
1	0·5819	0·6749	1·841	1·809
2	0·4865	0·5357	3·054	3·019
3	0·4344	0·4679	4·201	4·167
4	0·3997	0·4252	5·318	5·284
5	0·3741	0·3947	6·416	6·383
6	0·3541	0·3714	7·501	7·470
7	0·3379	0·3528	8·578	8·548
8	0·3244	0·3374	9·647	9·618

TABLE 4. Maximum values of $J_n(\xi)$ and asymptotic approximations for large n

REFERENCES

ALBERS, V. M. 1960 *Underwater Acoustics Handbook*, 290 pp. Penn. State Press.

BARTHOLOMEUSZ, E. F. 1958 The reflection of long waves at a step. *Proc. Camb. Phil. Soc.* **54**, 106–118.

BICKLEY, W. G. 1943 Formulae relating to Bessel functions of moderate or large argument or order. *Phil. Mag.* **34** (Ser. 7), 37–49.

BRYAN, G. H. 1890 On a revolving cylinder or bell. *Proc. Camb. Phil. Soc.* **7**, 101–111.

BUDDEN, K. G. 1961 *The Wave-Guide Mode Theory of Wave Propagation*. Englewood Cliffs, N.J.: Prentice-Hall, 325 pp.

CHAMBERS, Ll. G. 1965 On long waves on a rotating earth. *J. Fluid Mech.* **22**, 209–216.

DEBYE, P. 1909 Näherungsformeln für die Zylinderfunktionen für grosse Werte des Arguments und unbeschränkt veränderliche Werte des Index. *Math. Ann.* **67**, 535–558.

† For higher terms in this expansion see Olver (1954).

ECKART, C. 1950 The ray-particle analogy. *J. Mar. Res.* **9**, 139–144.

ECKART, C. 1951 Surface waves on water of variable depth. U.S. Office of Naval Research. Wave Rept. no. 100. (Notes of lectures given at the Scripps Institution of Oceanography).

GREENSPAN, H. P. 1956 The generation of edge-waves by moving pressure distributions. *J. Fluid Mech.* **1**, 574–592.

JEFFREYS, H. & JEFFREYS, B. S. 1950 *Methods of Mathematical Physics*, 708 pp, 2nd ed. Cambridge University Press.

KAJIURA, K. 1958 Effect of coriolis force on edge waves (2) Specific examples of free and forces waves. *J. Mar. Res.* **16**, 145–157.

LAMB, H. 1932 *Hydrodynamics*, 6th ed. Cambridge University Press.

LORENZ, L. V. 1890 Sur la lumière réfléchie et réfractée par une sphère transparente. *Vidensk. Selsk. Skrifter*, **6**, 1–62. (Original in Danish; French translation in *Oevres Scientifiques de L. Lorenz*, vol. 1, Copenhagen, Libraire Lehmann 1896; reprinted New York: Johnson 1964.)

MILLER, J. C. P. 1964 *The Airy Integral.* Brit. Ass. Math. Tables, Part-vol. B, 56 pp. Cambridge University Press.

MUNK, W. H., SNODGRASS, F. & CARRIER, G. 1956 Edge waves on the continental shelf. *Science* **123**, 127–132.

OLVER, F. J. W. 1954 The asymptotic expansion of Bessel functions of large order. *Phil. Trans* A **247**, 328–368.

RAYLEIGH, LORD 1945 *The Theory of Sound* 2nd ed., 504 pp. New York: Dover

REID, R. O. 1958 Effect of coriolis force on edge waves (1) Investigation of the normal modes. *J. Mar. Res.* **16**, 109–144.

SCHIFF, L. I. 1949 *Quantum Mechanics*, 409 pp. London: McGraw-Hill.

SNODGRASS, F. E., MUNK, W. H. & MILLER, G. R. 1962 Long-period waves over California's continental borderland. Part 1. Background spectra. *J. Mar. Res.* **20**, 3–30.

STOKES, G. G. 1846 Report on recent researches in hydrodynamics. *Br. Ass. Rept.* 1846; see also *Coll. Pap.* **1**, 167.

URSELL, F. 1951 Trapping modes in the theory of surface waves. *Proc. Camb. Phil. Soc.* **47**, 347–358.

URSELL, F. 1952*a* Edge waves on a sloping beach. *Proc. Roy. Soc.* A **214**, 79–97.

URSELL, F. 1952*b* Discrete and continuous spectra in the theory of gravity waves. Proc. Symp. on Gravity Waves, *U.S. Nat. Bur. Standards, Circular* 521, pp. 1–5.

WATSON, G. N. 1922 *A treatise on the theory of Bessel functions*, 804 pp. Cambridge University Press.